

Md Asifuzzaman Yen

**PROCESSING OF GRAPHENE OXIDE INTEGRATED
CELLULOSE ACETATE COMPOSITES AND THEIR
PHYSICAL AND MECHANICAL PROPERTIES.**

Faculty of Engineering Sciences
Master of Science Thesis
March, 2019

ABSTRACT

Md Asifuzzaman Yen: **Processing of Graphene Oxide Integrated Cellulose Acetate Composites and Their Physical and Mechanical Properties.**

Master's Thesis

Tampere University

Master's in Materials Science and Engineering

March, 2019

This thesis work deals with the fabrication of bionanocomposite films composed of cellulose acetate (CA) biopolymer and graphene oxide (GO) by melt extrusion process. Desired amount of triethyl citrate (TEC) was used as a plasticizer to produce flexible CA and CA/GO composite films. The GO 0.25, GO 0.5 and GO 0.65 composite samples were fabricated, where the numbers presented after GO indicate the weight % of GO with respect to CA. The TEC plasticized CA polymer film was also manufactured in similar way without using any GO for comparison purpose. GO was produced by the oxidation of graphite using modified Hummers method and used as a nano filler for composite manufacturing. Structural, thermal and mechanical properties of the TEC plasticized CA and CA/GO composite films were also explored in this thesis. Fourier Transform Infrared Spectroscopy (FTIR) and Differential Scanning Calorimetry (DSC) study of the composite films confirm the presence of the interfacial interaction between the GO and CA polymer chain. Wide Angle X-ray Scattering (WAXS) results and Scanning Electron Microscopy (SEM) images demonstrate that GO sheets are well dispersed into the CA matrix in GO 0.25 and GO 0.50 composite films, whereas prominent agglomeration of the GO sheets in CA matrix was observed in GO 0.65 composite film. Isothermal Thermogravimetric Analysis (TGA) curves show the lower mass loss of the composite films compared to the TEC plasticized CA film. Mechanical testing results show a noticeable increase of tensile strength and Young's modulus in the TEC plasticized CA/GO composite films compared to the TEC plasticized CA film.

Keywords: Bionanocomposite, Melt extrusion, Cellulose acetate, Graphene oxide, Triethyl citrate, Plasticizer, Tensile strength.

The originality of this thesis has been checked using the Turnitin Originality Check service.

PREFACE

This thesis work was performed in the Materials Science and Engineering Department of Tampere University.

I would like to thank Academy Postdoctoral Researcher Rama Kanta Layek, Assistant Professor Essi Sarlin and University Instructor Ilari Jönkkäri for giving me valuable feedback during my thesis work. I would like to appreciate Rama Kanta Layek for helping me with FTIR data as well as taking SEM images and assisting me with mechanical testing machine. I would like to thank Postdoctoral Researcher Gourab Saha for helping me with WAXS data. I would like to acknowledge Ilari Jönkkäri for instructing me to operate the Melt Extruder. I would also like to thank Research Assistant Clara Lessa Belone for the assistance with DSC and TGA measurements.

Tampere, 15.03.2019

Md Asifuzzaman Yen

CONTENTS

| | | |
|-------|---|----|
| 1 | INTRODUCTION..... | 1 |
| 2 | BIOPOLYMERS AND BIONANOCOMPOSITES | 4 |
| 2.1 | Biopolymers..... | 4 |
| 2.2 | Cellulose..... | 5 |
| 2.2.1 | Chemical Structure of Cellulose | 5 |
| 2.2.2 | Cellulose Derivatives..... | 5 |
| 2.3 | Cellulose Acetate | 6 |
| 2.3.1 | Properties of Cellulose Acetate..... | 7 |
| 2.4 | Plasticizers | 7 |
| 2.4.1 | Citrates | 8 |
| 2.5 | Composites..... | 8 |
| 2.5.1 | Bionanocomposites..... | 9 |
| 2.5.2 | Cellulose Based Bionanocomposites | 10 |
| 2.5.3 | Nano-Dimensional Particles..... | 10 |
| 3 | GRAPHENE | 12 |
| 3.1 | Synthesizing Graphene Oxide (GO)..... | 13 |
| 3.2 | Properties and Applications of Graphene Oxide | 14 |
| 3.3 | Reduced Graphene Oxide | 15 |
| 3.3.1 | Preparation of Reduced Graphene Oxide | 15 |
| 3.4 | Production of GO-Based Bionanocomposites..... | 16 |
| 3.4.1 | Solution Intercalation..... | 16 |
| 3.4.2 | Melt Processing..... | 16 |
| 3.4.3 | In Situ Polymerization | 17 |
| 4 | MELT MIXING METHOD OF POLYMER AND NANOPARTICLES | 18 |
| 4.1 | Polymer Extrusion | 18 |
| 4.1.1 | Single Screw Extruder..... | 19 |
| 4.1.2 | Twin Screw Extruder..... | 21 |
| 4.2 | Melt Extrusion of CA/GO Bionanocomposites..... | 22 |
| 5 | MATERIALS AND EXPERIMENTAL PROCEDURES | 23 |
| 5.1 | Materials | 23 |
| 5.2 | Process Flow of the Experimental Work..... | 24 |
| 5.3 | Synthesis of GO by Modified Hummers Procedure..... | 25 |
| 5.4 | Manual Grinding and Mixing of the Samples..... | 27 |

| | | |
|-------|---|----|
| 5.4.1 | Procedure for Sample Preparation | 27 |
| 5.5 | Processing of the Samples | 29 |
| 5.5.1 | Processing Procedure and Operating Parameter | 30 |
| 5.6 | Heat Pressing the Samples | 31 |
| 6 | CHARACTERIZATION OF MATERIALS | 33 |
| 6.1 | Fourier Transform Infrared Spectroscopy (FTIR) | 33 |
| 6.2 | Wide Angle X-Ray Scattering (WAXS) | 33 |
| 6.3 | Differential Scanning Calorimetry (DSC) | 34 |
| 6.4 | Thermogravimetric Analysis (TGA) | 34 |
| 6.5 | Field Emission Scanning Electron Microscopy (FESEM) | 35 |
| 6.6 | Mechanical Testing | 35 |
| 7 | RESULTS AND DISCUSSION | 36 |
| 7.1 | FTIR Results | 36 |
| 7.2 | WAXS Results | 38 |
| 7.3 | DSC Results | 39 |
| 7.4 | TGA Results | 41 |
| 7.5 | FESEM Images | 42 |
| 7.6 | Mechanical Properties | 44 |
| 8 | FURTHER RESEARCH | 46 |
| | CONCLUSIONS | 47 |
| | REFERENCES | 49 |

ORDER OF FIGURES

| | | |
|-------------------|---|-----------|
| Figure 1. | <i>Chemical Structure of Cellulose.....</i> | <i>5</i> |
| Figure 2. | <i>Molecular Structure of Cellulose Ester.....</i> | <i>6</i> |
| Figure 3. | <i>Molecular Structure of Cellulose Acetate.....</i> | <i>7</i> |
| Figure 4. | <i>Chemical Formula of Citrates.....</i> | <i>8</i> |
| Figure 5. | <i>Main Types of Polymer Composites.....</i> | <i>9</i> |
| Figure 6. | <i>Basic Nanostructures Based on Geometry.....</i> | <i>11</i> |
| Figure 7. | <i>Structural Arrangements of Graphene.....</i> | <i>12</i> |
| Figure 8. | <i>Preparation of Graphene Oxide.....</i> | <i>13</i> |
| Figure 9. | <i>Structural Comparison Of Graphite Oxide and Graphene Oxide.....</i> | <i>14</i> |
| Figure 10. | <i>Reduction Flow of Graphite Oxide and Graphene Oxide.....</i> | <i>15</i> |
| Figure 11. | <i>Flow of a Basic Extrusion Process.....</i> | <i>19</i> |
| Figure 12. | <i>Components and Zones of a Single Screw Extruder.....</i> | <i>20</i> |
| Figure 13. | <i>Co-rotating & Counter-rotating Screw System.....</i> | <i>21</i> |
| Figure 14. | <i>Interpenetrated and Non-interpenetrated Screw System.....</i> | <i>21</i> |
| Figure 15. | <i>Process Flow of the Experimental Work.....</i> | <i>24</i> |
| Figure 16. | <i>Pictures Taken during GO Synthesis.....</i> | <i>26</i> |
| Figure 17. | <i>Pure CA Sample Mixed with Triethyl citrate.....</i> | <i>28</i> |
| Figure 18. | <i>Manually Mixed Composite Samples.....</i> | <i>28</i> |
| Figure 19. | <i>Twin-Screw Extruder.....</i> | <i>29</i> |
| Figure 20. | <i>Processed Samples.....</i> | <i>30</i> |
| Figure 21. | <i>Heat Pressing Machine Setup.....</i> | <i>31</i> |
| Figure 22. | <i>Heat-pressed Polymer and Composite Samples.....</i> | <i>32</i> |
| Figure 23. | <i>FTIR Spectra of TEC Plasticized CA and CA/GO Composite Films.....</i> | <i>37</i> |
| Figure 24. | <i>WAXS of GO, TEC Plasticized CA & CA/GO Composite Films.....</i> | <i>39</i> |
| Figure 25. | <i>DSC Thermograms of TEC Plasticized CA and CA/GO Composite Films.....</i> | <i>40</i> |
| Figure 26. | <i>Isothermal TGA Curves of TEC Plasticized CA and CA/GO Composite films.....</i> | <i>41</i> |
| Figure 27. | <i>FESEM Images.....</i> | <i>43</i> |
| Figure 28. | <i>Stress-Strain Curves of TEC Plasticized CA and CA/GO Composite Films.....</i> | <i>44</i> |

LIST OF SYMBOLS AND ABBREVIATIONS

| | |
|----------------|---|
| FTIR | Fourier Transform Infrared Spectroscopy |
| WAXS | Wide Angle X-Ray Scattering |
| DSC | Differential Scanning Calorimetry |
| TGA | Thermogravimetric Analysis |
| FESEM | Field Emission Scanning Electron Microscopy |
| CA | Cellulose Acetate |
| GO | Graphene Oxide |
| rGO | Reduced Graphene Oxide |
| DP | Degree of Polymerization |
| CAP | Cellulose Acetate Propionate |
| CAB | Cellulose Acetate Butyrate |
| TEC | Triethyl Citrate |
| T _g | Glass Transition Temperature |
| VDW | Van Der Waals |
| <i>d</i> | distance |
| λ | wavelength |
| θ | diffraction angle |

1 INTRODUCTION

Plastics derived from petroleum resources are used widely for variety of demanding applications such as electronics, household items, packaging films, trash bags, medical devices and packaging of preservable products [1-3]. The usage of these petroleum based plastics is very high owing to their excellent mechanical properties and gas barrier properties [4]. However, only a small amount of these plastics from the used products are reprocessed or reused and most of it end up being dumped in the soil and seas of the nature which increases environmental pollution [5, 6]. Due to this threat to the environment, continuous approaches and researches are being made towards substituting petroleum based plastics with biodegradable polymers. Therefore, the biodegradability of biopolymers comes across as an environmental attribute more than its functional necessity. Biopolymers, also known as natural polymers, are formed in the nature. Since biopolymers endure bond scission in their polymer chain through the action of natural microorganism, they become disintegrated and degraded in the nature. [7, 8]

Among all the biopolymers, polysaccharide cellulose is one of the most common and useful polymeric raw materials having remarkable structure and characteristics. It is characterized by hydrophilicity, bio-degradability and chemically modifying capacity. However, the attraction of cellulose biopolymer is chiefly due to the multi functionality and stiffness in the polymer chain. Cellulose can be chemically altered to cellulose esters for the ease of film formation. Cellulose derivatives can be used to make bionanocomposites with the judicious integration of suitable nanoparticles. Chemically modified cellulose is suitable for manufacturing packaging materials for different products. [9, 10]

Cellulose acetate (CA) is known to be one of the most significant derivatives of cellulose [11]. Recent studies by Bao et al. (2015) have shown the possibility to make flexible CA film by **solvent casting** using suitable plasticizer. However, the solvent casting process is not suitable for large volume manufacturing and industrial applications. [12] Although there are some restrictions to process cellulose derivatives as polymer films by melt extrusion due to their degradability before melting point, Jeon et al. (2012) in their study have successfully produced Cellulose Acetate Propionate (CAP) neat and composite films [13]. In a study of Quintana et al. (2012), it is found that citrate based plasticizers,

for instance, environment friendly triethyl citrate (TEC) has proved to be the most appropriate to use with CA [14]. The use of a suitable plasticizer ensures the reduction of glass transition temperature (T_g) and melting point of CA which increases melt processability [15, 16, 17]. However, the inherent properties of CA as a biopolymer such as mechanical weakness and high gas permeability restricts its potential applications in various fields [18]. According to Ojijo and Ray (2013), continuous efforts are being made over the past few years to develop bionanocomposites by intruding nanoparticles such as graphene, carbon nanotubes, silica, clay etc. into the biopolymer matrix to enhance the overall properties of the resultant material [19].

Carbon based nanoparticles have very low density and they assist ease of processing of the polymer composite material. A high aspect ratio is necessary to provide a considerable reinforcing efficiency. Hence, graphene oxide (GO) having a very high aspect ratio, increases the mechanical properties such as, tensile strength and stiffness of the polymer composite material. GO can be synthesized through oxidation of graphite. [20] Researches conducted by Uddin et al. (2016) and Carlos Avila-Orta et al. (2017) illustrate the preparation of CA/GO & starch/GO bionanocomposites respectively with the incorporation of GO nano sheets which significantly improved the mechanical characteristics of the resultant composite films [21, 22]. However, most of the researches including the above mentioned studies to manufacture GO integrated biocomposites focus on **solvent casting** method which is not compatible for industrial use [22]. Hence, this thesis focuses on manufacturing CA/GO bionanocomposite films through **melt processing**.

The main objects of this research work are to produce CA polymer film and CA/GO bionanocomposite films using TEC plasticizer through melt processing as well as to characterize and analyze different properties of the films, for instance, structural, thermal and especially mechanical properties. The methodology intended for the processing of biopolymers and composites on a large scale by solvent casting has not yet been established. Thus, emphasis has been given to discover whether flexible CA/GO composite films treated with TEC plasticizer can be manufactured through **melt extrusion** since it is considered a suitable method for processing bulk polymer and composite materials in the industrial sectors. Again, melt processing will also ensure the absence of solvents in the composite films which will be more eco-friendly. Furthermore, the possibility of enhanced **mechanical properties** of the TEC plasticized CA/GO melt extruded composite films is a significant motive to conduct this work. In this thesis, the attention has been given for the escalation of the mechanical properties of the TEC plasticized CA/GO

bionanocomposites discounting gas barrier property which is also an essential attribute for packaging applications.

The whole thesis work has been divided into two sections, theoretical and experimental. The theoretical part focuses on properties and classification of biopolymers as well as properties and molecular structures of cellulose and CA. Furthermore, a general overview of plasticizers, bionanocomposites and nanoparticles has been illustrated. A separate chapter introduces and explains molecular structure, synthesis, properties and applications of GO. In addition, different methods for producing bionanocomposites have also been discussed afterwards.

The experimental segment illustrates the whole process flow, procedure for sample preparation and synthesis of GO. Moreover, the methods to characterize the produced samples have been briefly discussed. Lastly, the results obtained from the characterization methods have been analyzed and the outcome has been discussed in the conclusion part.

2 BIOPOLYMERS AND BIONANOCOMPOSITES

2.1 Biopolymers

Biopolymers consist of natural biopolymers and synthetic biopolymers. The modification and development of synthetic biopolymers have increased a diversity of applications in different fields [23]. All the natural biopolymers or in other words, biodegradable polymers can be capable of getting decomposed with the action of water, carbon dioxide or enzymatic action of micro-organisms. Biodegradable polymers can be bio-based and fossil fuel based. [24] Bio-based and fossil energy based bio decomposable polymers are illustrated in Table 1.

Table 1. *Biodegradable polymers categorized into Bio-based and Fossil energy based [24]*

| Origin | Biodegradable Polymers |
|---------------------|---|
| Bio-based | Cellulose acetate, cellulose acetate butyrate, polylactic acid, starch, chitosan etc. |
| Partially bio-based | Polylactic acid blends and starch blends |
| Fossil fuel based | Polybutylene succinate, polycaprolactone, polyvinyl alcohol etc. |

Since, the mechanical and the barrier properties for the end material is very important, lot of researches have been going on to make biodegradable polymer films using nano-fillers to make it mechanically strong and inserting excellent barrier properties in the biopolymer composite material. Few of the biodegradable polymers can be obtained from the market, for instance- CA, polylactic acid, starch and blend of starch. By using biopolymer films in place of synthetic plastic materials, the waste disposal system of the end materials can be easier. [25]

Two notes that can be considered in support of biopolymers:

- The opportunity to stop the carbon cycle to the soil by means of bio-degradation and because of that lessening the environmental impact,
- Limited use of fossil energy and less emission of carbon dioxide based on the life phase of the product that is produced. [26]

2.2 Cellulose

Among all the biopolymers, polysaccharide cellulose is one of the most common and useful polymeric raw materials having excellent structure and characteristics. The structure is formed by the repetition of D-glucose units. It can be chemically modified to cellulose esters and that can be used to make bionanocomposites with the addition of suitable nano fillers. The attraction of cellulose biopolymer is mainly due to the particular structure of the polymer. Cellulose is different as compared to synthetic polymer based upon mainly on its multi functionality and stiffness in the polymer chain. [9] Chemically modified cellulose can be used to produce biodegradable polymers that can be utilized to manufacture packaging materials for different products and plastics [10].

2.2.1 Chemical Structure of Cellulose

The degree of polymerization (DP) estimates the chain length of cellulose. The DP differs with the raw material. It is around 300-1700 and for the regenerated cellulose, the DP varies from 250-500 per chain. The cellulose chain polymer comprises D-glucose unit at one end with genuine C4-OH group. The other end is bounded with genuine C1-OH group, known as the reducing portion. The structure of cellulose gives it the advantage of hydrophilicity, degradability and reactivity because of the existence of -OH groups in the polymer chain. [9]

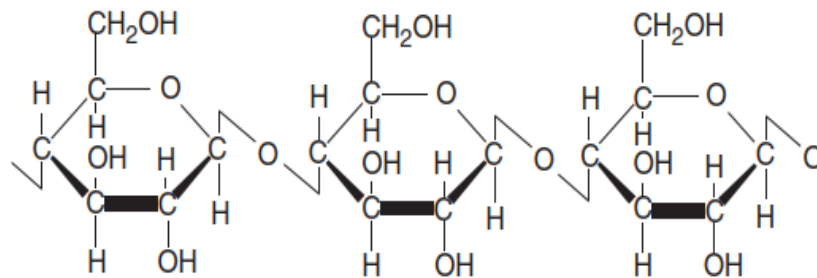


Figure 1. Molecular Structure of Cellulose [9].

2.2.2 Cellulose Derivatives

Cellulose derivatives are normally chemical modification of cellulose. Cellulose derivative can be of two types- cellulose ethers and cellulose esters. Cellulose esters normally have high stiffness, low ductile nature, good transparency, decent thermal and impact resistance. However, the biodegradability of cellulose derivatives or esters depends upon the degree of substitution. The degree of substitution also known as the acetylation level refers to the replacement of the hydroxyl groups with acetyl group in the cellulose

ester structure. When the grade of substitution is high, the polymer is degraded at a very slow rate. But, when the degree of substitution is lower, the cellulose derivatives tend to degrade in the microorganism or in any media of nature at a comparatively faster pace. [12, 24] Cellulose esters are very advantageous polymers having biodegradability. The main applications of cellulosic esters are photographic films, medical field, automotive coverings, toothbrush handles. As illustrated in Figure 2, the chemical structure of cellulose ester constitutes of a) cellulose acetate (CA), b) cellulose acetate propionate (CAP) and c) cellulose acetate butyrate (CAB). [27]

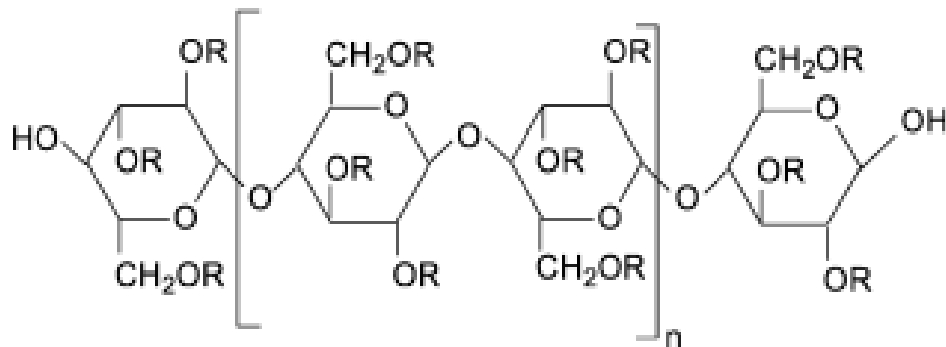


Figure 2. Molecular Structure of Cellulose Ester [27].

2.3 Cellulose Acetate

The ester of cellulose is known to be cellulose acetate (CA). When cellulose is reacted with acetic acid and then with acetic anhydride with involving a reagent, for instance, sulfuric acid, it can produce CA. As soon as the cellulose gets fully acetylated, it is known as cellulose tri-acetate. This compound polymer is a crystalline substance having almost 250 °C melting temperature. However, the acetylation of cellulose causes the hydrogen of the hydroxyl groups (-OH) to be replaced by the acetyl groups (CH₃-CO). [11] CA has the applications in textile, photographic film, materials engineering industry, cigarette and other filters [24]. Since, CA is not thermoplastic itself, it is decomposed below the melting temperature. But, CA can be processed by melt extrusion with the addition of a suitable plasticizer. The more the amount of plasticizer is used on the weight of CA, the T_g gets lower. Consequently, the decreased T_g leads to more free volume in the polymer chain of the resultant material. Use of suitable plasticizer of desired weight percentage reduces the complexity of melt processing to decent extent. However, the most commonly used plasticizers with CA are di-ethyl phthalate, tri-acetine, tri-ethyl citrate etc. [15] The role and mechanism of plasticizers will be discussed in more detail later in the “Plasticizers” segment.

2.3.1 Properties of Cellulose Acetate

CA demonstrates rigid mechanical behavior and high Young's modulus. In comparison to cellulose, CA has lesser hydrophilicity and thus higher water vapor barrier property because of the lower amount of hydroxyl (-OH) groups that are present in the polymer structure. Nevertheless, CA still is more gas permeable than the other petroleum founded plastics. Thermal characteristics for instance-glass transition temperature (T_g) and melting point are very important factors for the processing of CA biopolymer. Since, CA has very high glass transition temperature (around 340K); it is very challenging to process this polymer by melt extrusion. Due to this purpose, plasticizers with low molecular weight are mixed with the basic polymer, which makes the material melt processable without getting degraded. [28]

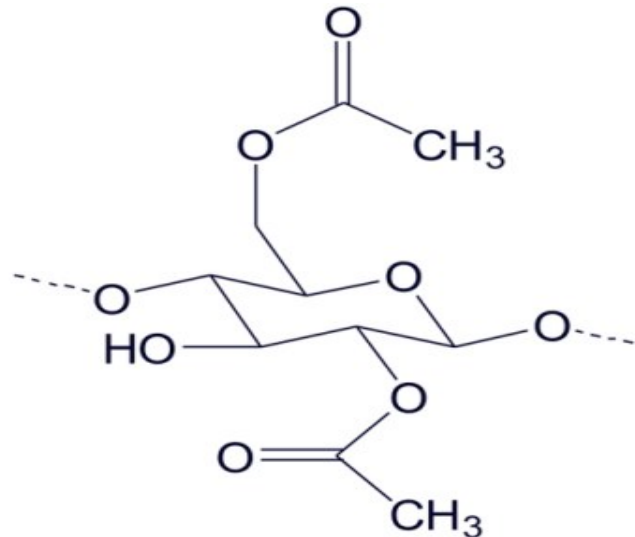


Figure 3. Molecular Structure of Cellulose Acetate [28].

2.4 Plasticizers

Plasticizers having a very low molecular weight and no volatility at all are normally used vastly in the polymer industries. The main objective of using plasticizers with the polymers are to enhance the ability to process the polymers and to make the polymer flexible enough by the reduction of glass transition temperature. Plasticizers having low molecular size assists to obtain intermolecular spaces or rooms between the chains of the polymer, which lessens the secondary forces among them. Plasticizer can normally be internal or external plasticizers. External plasticizers can be removed from the polymer

by evaporation, as there are no chemical attachment to the polymer chain by strong bonds. Internal plasticizers normally become the parts of those specific polymers with which they are treated. There are also primary and secondary plasticizers. In primary plasticizers, high concentration of polymer is soluble. On the other hand, secondary plasticizers are characterized by low compatibility with the polymer. Most common commercially available classic plasticizers are phthalate esters, adipates, citrates etc. [29] Plasticizers not only have an effect on the gelation temperature, but also they can reduce the melting temperature of the polymer and thus improving the processability of the material with lower degradation temperature and reduced mixing time [16].

2.4.1 Citrates

Ethyl, butyl, acetyl and stearyl citrates are most common among all citrates. The citrates are very much suitable for cellulose, CA, PVA, PVB etc. [30]. The general chemical formula of commercially available citrates is demonstrated in Figure 4.

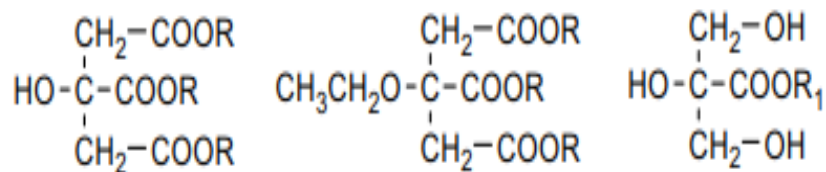


Figure 4. Chemical Formula of Citrates, R_1 = stearyl, R = ethyl, butyl or hexyl [30].

When phthalate plasticizers are used commercially for processing of cellulose esters, they can pose a considerable environmental threat while using for long period. However, the citric acid is used for flavoring food. The ester of citric acid can be used as a plasticizer for the processing of various polymers as well as for different applications such as contact with food and medical application. Using of environmental friendly triethyl citrate as a plasticizer for CA to make it processable gives a better opportunity to make a more eco-friendly bio-plastic. [17]

2.5 Composites

Composites are manufactured from two or more elements that have different set of mechanical properties remaining separate and discrete in their finished structure. There are normally two parts of the composite materials: matrix and reinforcement. The matrix en-

virons and backs the reinforcement by helping them to hold their positions. The reinforcement strengthens the matrix by enhancing the mechanical features of the composite material. [31] Composites are formed when micro sized organic/inorganic additives are combined with the synthetic plastic materials. The micro-sized inorganic additives can be carbon black, talc, calcium carbonate etc. Difference between a composite and nanocomposite can be found out by the size of the inorganic additives. If the inorganic additives are in the nano sized state, it is known as a nanocomposite material. Nanocomposites and bionanocomposites can only be differentiated by considering several facts such as: their solubility in water, biodegradability and thermal stability. [32] The main types of polymer composites based on their constituents are demonstrated in Figure 5.

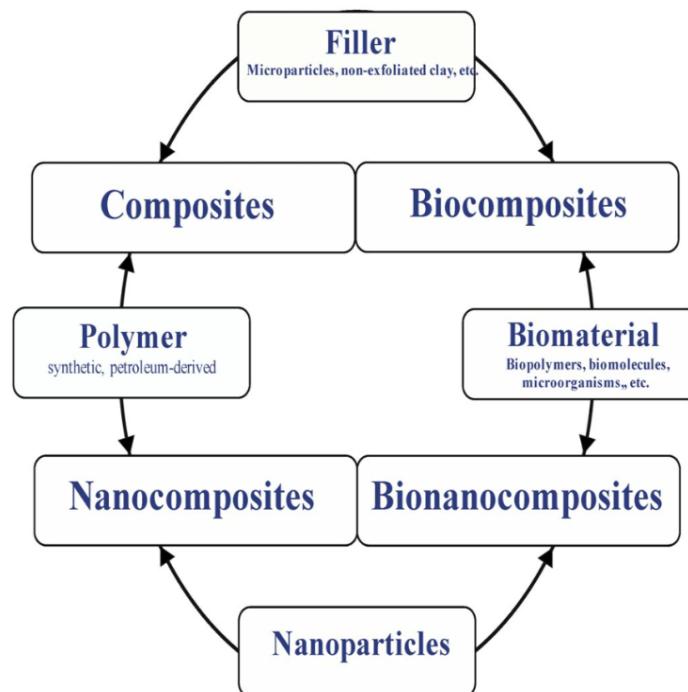


Figure 5. Main Types of Polymer Composites [32].

2.5.1 Bionanocomposites

Biopolymers are being used recently for the making of bionanocomposites. The main reason behind using biopolymers instead of petroleum-based plastics is the ecological and environmental safety. Natural polymers have the significant property of biodegradability through the action of naturally occurring microorganism. However, construction of nanocomposites from biopolymers such as cellulose and cellulose derivatives is an issue

in progress on which many experiments and researches have been going on for years. In the bionanocomposites, nano sized fillers having a size of 1-100 nm in at least one direction are mixed with the biopolymer matrix. This combination helps boost the strength and mechanical characteristics and resist the permeability of the bionanocomposite material. [33]

2.5.2 Cellulose Based Bionanocomposites

The matrix portion of a bionanocomposite constitutes of cellulose or cellulose derivatives. The nature of the matrix segment can be thermoplastic or thermosetting. Derivatives of cellulose such as CA can be processed in the same way as other plastics by melt extrusion by the addition of plasticizers of suitable amount. CA has the benefit of processing ease when compared to cellulose. They can be processed and made into a nanocomposite material with the addition of suitable nanoparticles or nanofibers or nano sheets. Triethyl citrate can be used as plasticizer with CA. Plasticized CA can be melt extruded as a bionanocomposite material with the incorporation of graphene or GO nano sheets at a sufficient temperature. [34]

2.5.3 Nano-Dimensional Particles

Nanoparticles are intruded into the matrix of the biopolymer with a view to mainly reinforcing the material. Nanoparticles also effect the physical properties of the biopolymer matrix. Dimensional stability, surface properties, biodegradability and processability of the biopolymer material also change to some extent. The nano sized particulates vary in shape and measurement. They have large surface area and the surface area gets increased with the reduction in the measurement or dimension of the particulates. The surface area of nanoparticles helps to make better contact with the biopolymer matrix molecules in the composite material. [33] From the Figure 6, we can see that nanostructured particles can be classified into 0-D, 1-D and 2-D nanomaterials based upon their dimensions.

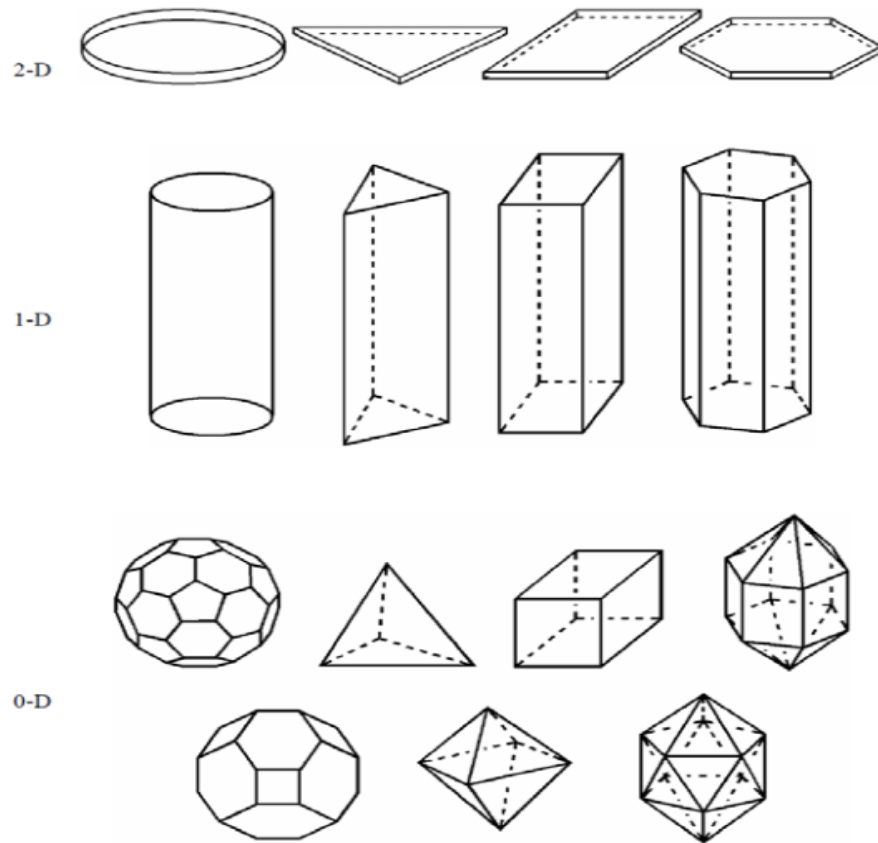


Figure 6. Basic Nanostructures Based on Geometry [35].

A thin film can be a two dimensional nanomaterial, if only the thickness of it is nano-sized. This grouping has been done according to the number of dimensions, which are not within the nano-sized zone. Zero dimensional nanostructured materials are referred as nanoparticles of which each dimension is under 100 nm. They are normally spherical shaped nanoparticles. Nano discs, nano plates and nano sheets are 2D-nanoparticles since two of the axis are totally extended except the thickness along one axis is in between the size of 1-100 nm. [35]

Graphene is known as two dimensional nanomaterial. The spacing between the sheets of graphene is 0.3 to 0.7 nm. Carbon nano sheets such as, GO, has an extremely thin two dimensional structure having oxygen containing functional groups. GO nano sheets have excellent stiffness and strength due to the 2D graphene backbone. Because of possessing high surface area, GO provides excellent reinforcing proficiency to the polymer matrix. [20] More about graphene and GO as well as their structure and properties will be discussed thoroughly in the next chapter “Graphene”.

3 GRAPHENE

Graphene is basically made of mono-layer of the atoms of carbon. The atomic structure of carbon in graphene remains in hexagonal shaped manner. Graphene is the most recent allotrope of carbon, having excellent strength yet decent flexibility. [36] Normally, sp^2 bonded carbon atoms are densely attached to each other producing a honeycomb array in the single atomic graphene layer. It is the rudimentary fundamental constituent of all other graphite materials. [37] Graphene exhibits excellent electronic and magnetic properties. Graphene can be used to reinforce polymer matrix by increasing the mechanical properties of the composite material. All these interesting properties of graphene has made it an innovative material for the future. [38] Production of graphene is carried out based on the properties required for particular applications. There are various procedures to produce graphene based on the required application of the products. For composite materials, graphene or graphene oxide is used. [39]

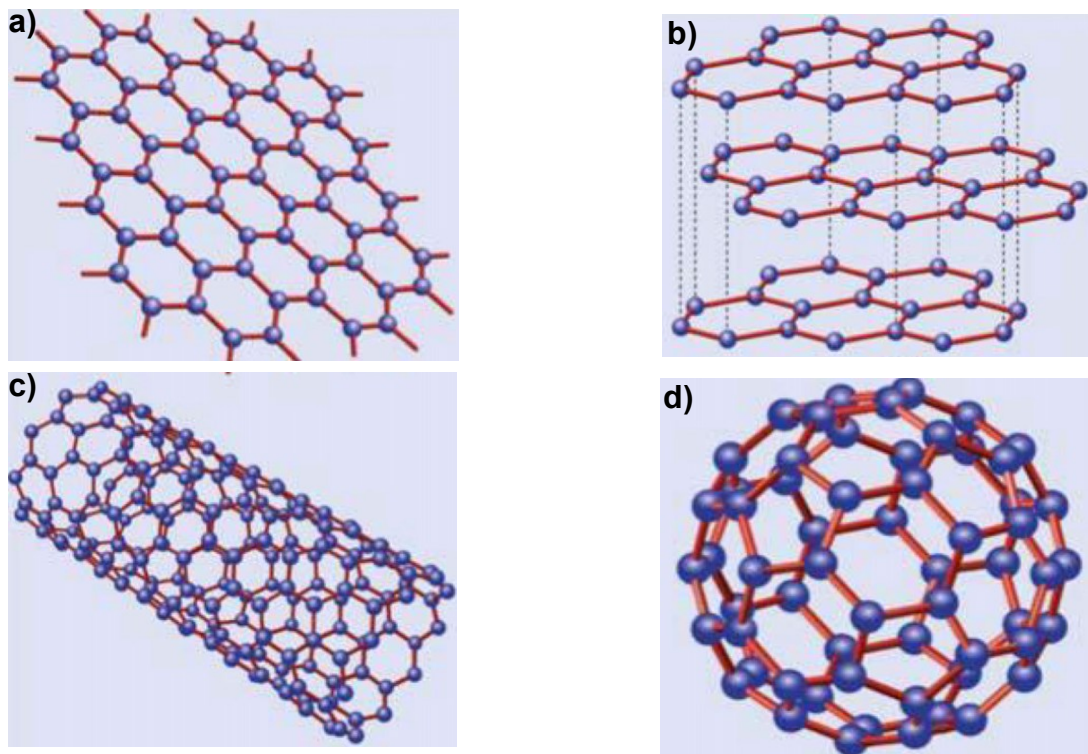


Figure 7. Structural Arrangements of Graphene: a) Graphene-honeycomb arrangement of carbon atoms, b) Graphite-piled layers of graphene, c) Carbon nanotubes-piled up graphene tubes, d) Wrapped graphene [40].

3.1 Synthesizing Graphene Oxide (GO)

GO is basically produced using Hummers procedure. Graphite is reacted with concentrated acid like H_2SO_4 and oxidizing agent for instance, KMnO_4 to yield graphite oxide. Graphite oxide contains functional groups based on oxygen for instance- hydroxyl, carboxylic and epoxy functional groups. Presence of hydroxyl and epoxy groups is very highly concentrated in graphite oxide. On the other hand, carboxylic groups are present in the boundary of the sheets. [41]

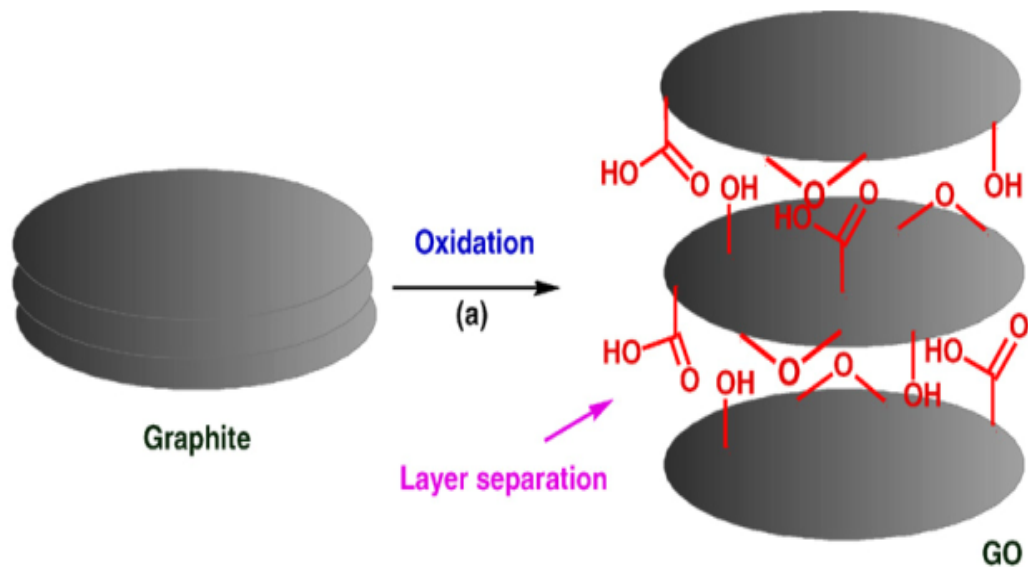


Figure 8. Preparation of Graphene Oxide [40].

Graphite oxide can be mechanically or chemically exfoliated. Graphite oxide is mechanically exfoliated with sonication process to yield GO, an extremely oxidized version of graphene. When graphite oxide is exfoliated into GO via sonication, the interlayer spacing between the sheets gets increased. The chemical arrangement of graphite oxide and the difference in the interlayer spacing between sheets in exfoliated GO is demonstrated in Figure 9. [41] The interlayer spacing in graphite is 0.335 nm and it gets increased to 0.625 nm for exfoliated GO [42].

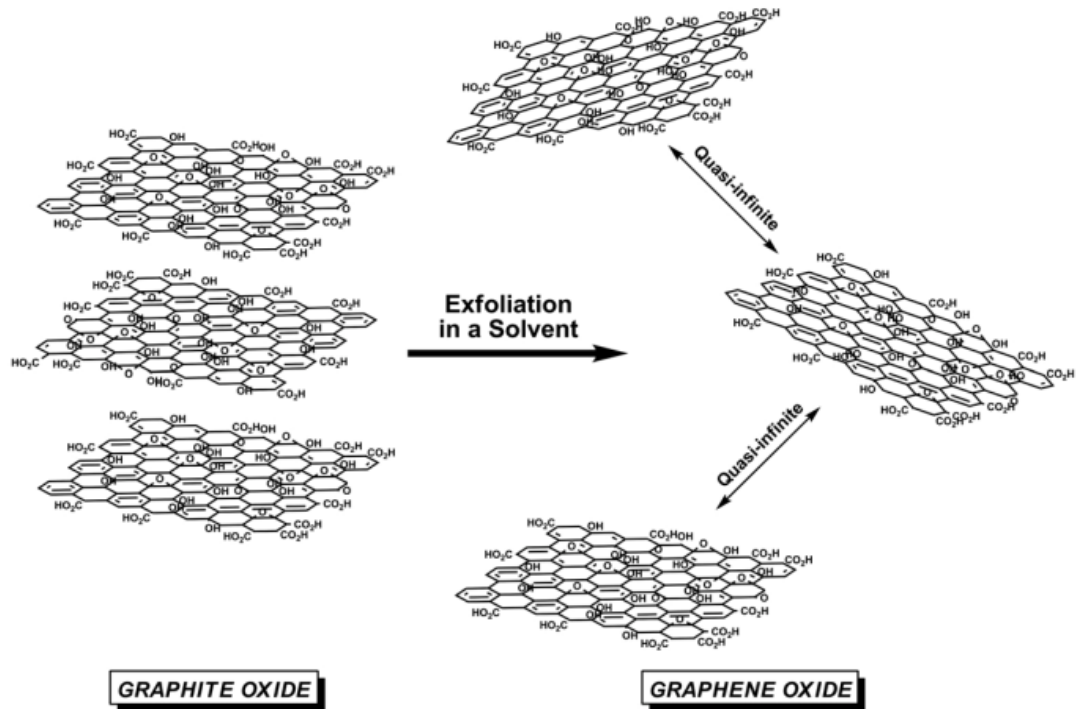


Figure 9. Difference in Structure between Graphite Oxide and Graphene Oxide [41].

Despite the usefulness of the Hummers method to produce GO, there are couple of obvious problems related to this process. They are, large consumption of oxidizing agents for the oxidation reaction and longer process period. [43]

3.2 Properties and Applications of Graphene Oxide

Since different functional groups based on oxygen remain in the GO structure, it displays a set of outstanding properties. They include thermal, mechanical, electronic and optical properties. GO sheets demonstrate good conductivity and photoluminescence. Oxygen-based functional groups in the GO structure make it chemically very active. It is noticed that the most significant chemical reaction for GO is reduction. GO can be reduced with the presence of a reductant at specific temperature. The most common reducing agent used for the reduction of GO is hydrazine. [44] Graphene based nanoparticles are useful to manufacture polymer nanocomposites for various applications. Polymer nanocomposites based on GO nano sheets have shown excellent mechanical & thermal characteristics, tensile properties and Young's modulus. [45]

3.3 Reduced Graphene Oxide

Oxidizing graphite chemically produces GO, which has oxygen containing chemical groups in the molecular structure. Reduction of GO is carried out with a view to reducing these oxygen containing functional groups to some extent. Reduction of GO can be performed by using different reducing agents for instance, dimethyl hydrazine, hydrazine, sulfur containing compounds, aluminum powder, ethylene-diamine etc. [46] Reduced Graphene oxide (rGO) has partial characteristics of graphene. The rGO sheets are considered as chemically modified or derived graphene. The aim of the reduction process is mainly to manufacture a material very close to pristine graphene. Chemical reduction of GO yields a partially reduced graphene oxide since the full reduction is not possible to achieve. A suitable reduction method gets rid of almost all of the oxygen based functional assemblies in a GO sheet. [47]

3.3.1 Preparation of Reduced Graphene Oxide

Distilled water is mixed with GO manufactured from modified Hummers method. A suspension of the mixtures is produced by sonication process in a water bath for couple of hours. Hydrazine monohydrate of suitable amount is added consequently to the mixture. The mixture is covered and kept at 85 °C for about 12 hours with continuous magnetic stirring. The mixture turns from brown to black, which confirms the execution of the reduction. Cooling of the mixture at room temperature is performed and it is dried for a day to yield rGO, which is normally collected using a surgical knife. [48]

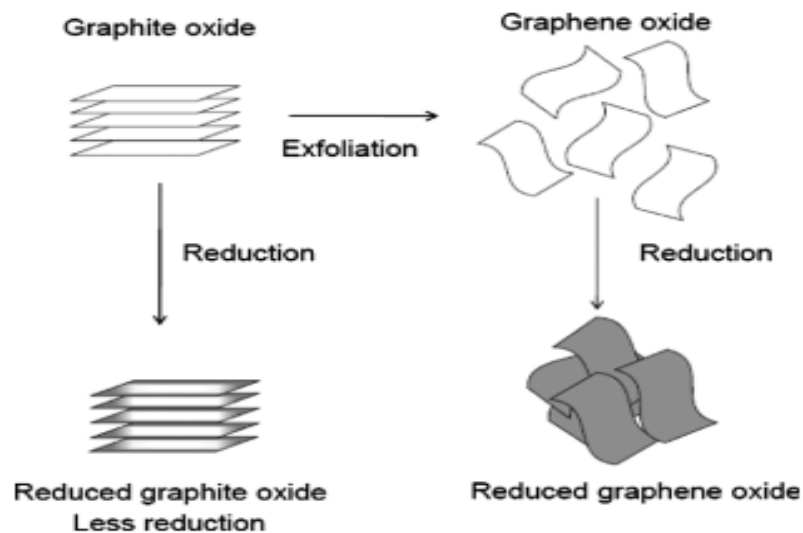


Figure 10. Reduction Flow of Graphite Oxide and Graphene Oxide [48].

3.4 Production of GO-Based Bionanocomposites

The processing and interaction between GO and biopolymer to produce bionanocomposites depends on several factors, such as, molecular weight, polarity and reactive groups present in the polymer. It is possible to make the best use of the nano-sized materials when the nanoparticles are completely uniformly distributed in the matrix of the polymer. The consistent and regular dispersion of the GO nano sheets can occur with the selection of a suitable processing method. There are normally three processing methods to produce GO based bionanocomposites. [31, 40]

3.4.1 Solution Intercalation

Basically, a suitable solvent system is mainly related with solution blending. Dispersion of GO based nano sheets can be done in a suitable solvent for instance, chloroform, H₂O, acetone etc. After that, it is mixed with the polymer solution. As soon as the solvent gets evaporated from the mixture, the sheets reconvene by integrating with the polymer to form nanocomposite. This approach is normally followed for the manufacturing of epoxy based nanocomposites. In this process, the removal of solvent is a very critical fact. The entropy achieved from the desorption of the solvent is an important driving issue for this processing method. For accepting the entering polymer chains, the filler content has to desorb most of absorbed solvent molecules. Polymer nanocomposites with the polymer having very low polarity can be produced or processed by the solution intercalation process. [40]

3.4.2 Melt Processing

In this technique, GO or chemically altered GO is mixed with the polymer matrix while still in melted phase. GO nano sheets are blended with the polymeric material and heated beyond the softening point of the polymer in a melt extruder with single or twin-screw method. This process has several benefits over the other processing techniques. First advantage is that this process is carried out without using any solvent. Secondly, melt mixing is compatible with the recent industrial production techniques for instance, melt extrusion or injection molding. Formation of bionanocomposites is possible with the melt processing technique, which is not suitable in the in situ polymerization process. The thermodynamic collaboration between the polymer and the nanoparticles mainly effect the formation of bionanocomposites by means of melt processing technique. The nanoparticles should properly spread in the matrix of the polymer composite for obtaining a

uniform bionanocomposite film. The intensity of dispersion between polymer matrix and the nanoparticles can be estimated with two important factors. [19, 40] They are,

- The enthalpic interaction that occurs between the nanoparticles and polymer matrix during melt processing,
- The conditions of melt processing, such as- time, temperature, speed etc.

The bionanocomposite can get degraded during processing if the processing temperature and time are not properly optimized. [19, 40] Melt blending can be a suitable method for the processing of a biopolymer like CA since it is compatible with a few number of solvents. CA can be processed with a suitable plasticizer like triethyl citrate. Plasticized CA when gets processed makes very useful and effective bioplastic that can be used in medical and automotive field. Plasticized CA and GO nano sheets can be processed together by means of melt processing technique to yield bionanocomposite that has the potential to have excellent applications in various fields. [14]

In the next chapter, different melt extruders and melt processing of biopolymers and composites have been discussed with elaboration.

3.4.3 In Situ Polymerization

This polymerization process is appropriate for the production of those polymer nanocomposites, the polymers of which have solubility problems in solvents or have thermal instability. In situ polymerization involves the pre-mixing of nanoparticles with monomer solution. An appropriate initiator is diffused in the solution. Later, by means of heat or radiation, the polymerization process is started. Graphene based nanoparticles can have a decent level of dispersion through in situ polymerization including a previous exfoliation. Monomers can also be intruded in between the layers of GO and later the polymerization process is carried out to discrete the layers. [19, 41]

4 MELT MIXING METHOD OF POLYMER AND NANOPARTICLES

Thermal properties of polymeric materials effect the processing outcome of the polymers. The thermal properties are mainly melting temperature of the polymers, T_g , temperature of degradation, thermal diffusion and thermal conduction. During the processing period, mechanical, thermal, visual and other properties are properly adjusted. Polymer extrusion is considered to be one of the most important methods for the processing of polymer. Extrusion of polymers have the below mentioned operational flow. [49]

- Polymer heating and melting,
- Polymer forcing to the shape-forming zone,
- Giving the polymer melt the necessary shape,
- Cooling the material and
- Solidification of the melt polymer. [49]

4.1 Polymer Extrusion

One of the most significant and essential methods for the processing of polymers and producing polymer composites is polymer extrusion. Extrusion of polymers increases the strength of the material along the polymer chain as well as the stiffness of the material. Extrusion process involves- solid transportation, melting of polymers, mixing the polymers, venting and homogenization. Single screw extruder and twin-screw extruder can carry out extrusion of polymeric materials. [49] The screw arrangement can be modularized as well as the process variables can be altered. These parameters make it likely to optimize processing parameters such as, temperature, speed, residence time etc. [50]

Before the extrusion processing, the polymers can be blended or mixed with additives such as plasticizers, heat stabilizers as well as fillers and reinforcements to yield the end material specific required properties and to make the processing conditions suitable for the processing of the polymer. The polymer mixed with suitable additives or fillers or reinforcements is dried properly in the curator before it is fed inside the extruder. In the extruder, the polymer preparation is melted, metered and transported to the die to give shape to the extrudate. After the material leaves the die, the polymer is cooled in room

temperature and solidified. Some secondary procedures such as flame treatment, printing and cutting can be carried out afterwards before the final inspection and packaging. [51]

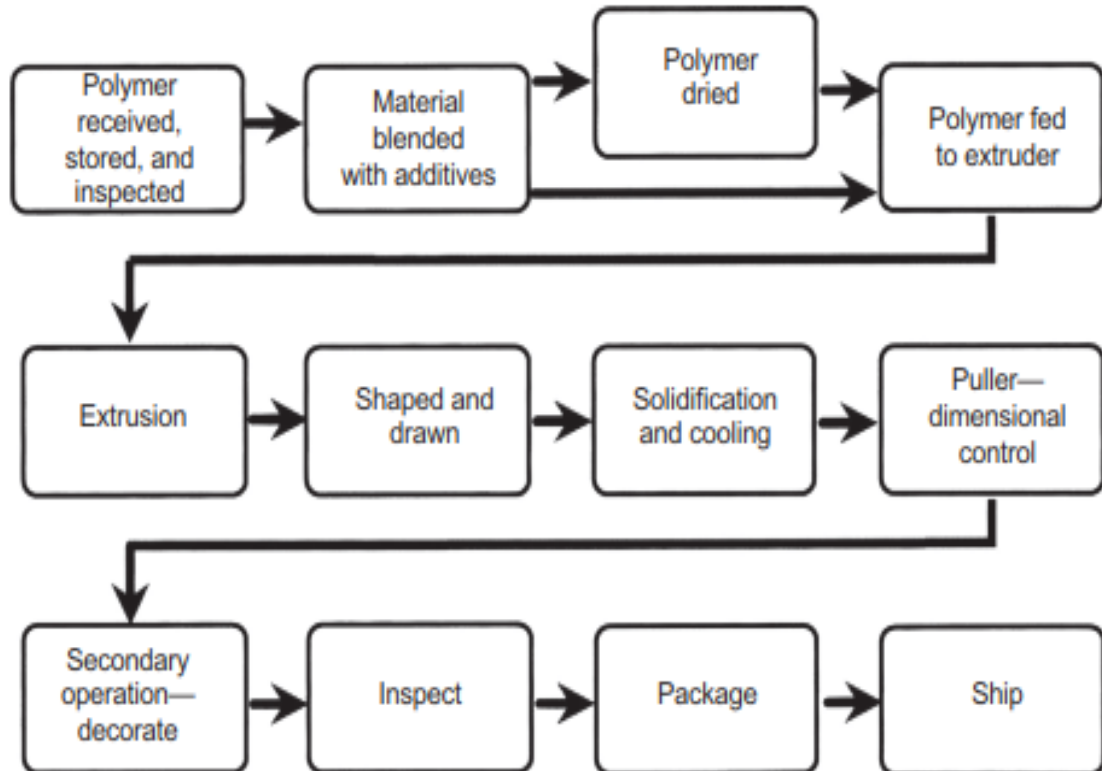


Figure 11. Flow of a Basic Extrusion Process [51].

4.1.1 Single Screw Extruder

An extruder with a single screw can be divided regarding functional and geometric sections. Feed section, compression section and metering section are the three geometric parts of a single screw extruder. Each part has different functions. [52] The basic constituents of this type of extruder has been illustrated in Figure 12.

Basic Operation of a Single Screw Extruder

Along the feed section, the polymer goes through the hopper. The material moves downwards to the barrel of the extruder from hopper. The material is placed in the room between the screw and the barrel. Since the barrel remains fixed and the screw keeps revolving, there are frictional forces acting on the polymer material, which keep the material moving further ahead. [52, 53]

The polymer material gets heated up from the heat originated by the frictional forces and the conducting heat generated from the barrel heaters. The solid conveying zone ends and the plasticating zone begins, as soon as the temperature rises above the melting point and a melt film forms at the surface of the barrel. [52, 53]

The quantity of solid material gets reduced due to the melting of the material. As soon as the entire solid polymer is vanished and all of it becomes molten, it indicates the ending of the plasticating zone and the beginning of the melt transporting zone where the molten polymer transports to the die. While flowing through the die, the molten polymer gets the exact shape of the flowing channel of the die. [52, 53]

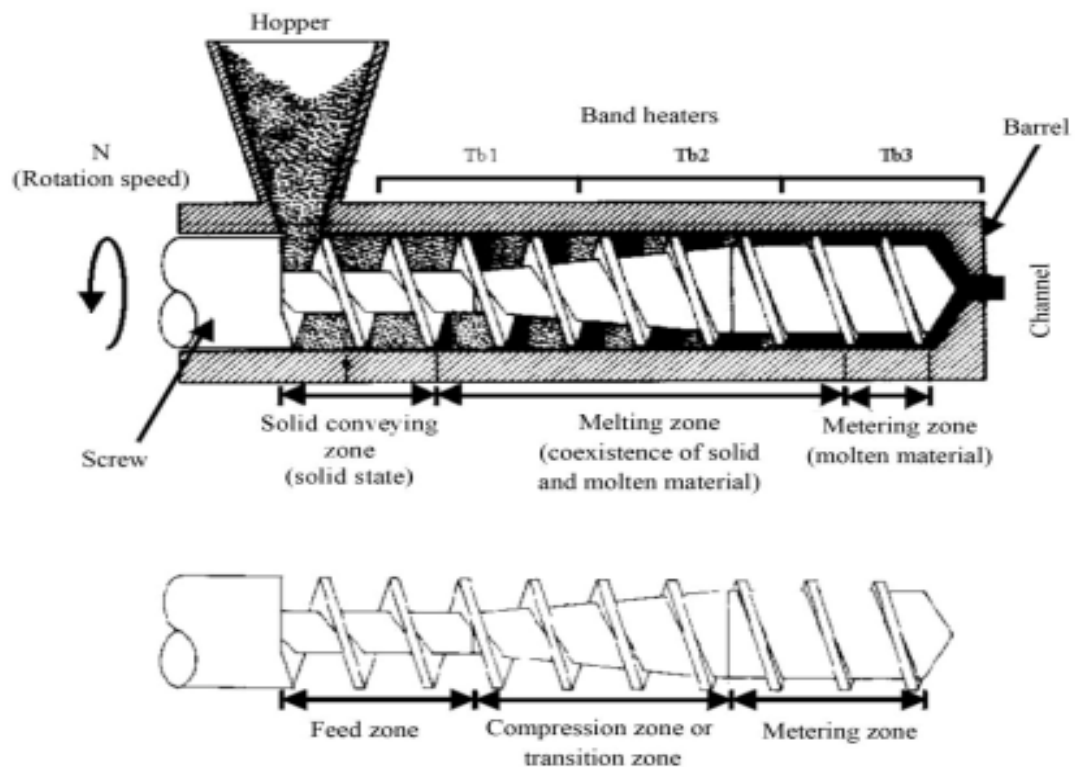


Figure 12. Components and Zones of a Single Screw Extruder [52].

4.1.2 Twin Screw Extruder

The key fact that differentiates the twin screw extruder from the single screw extruder is the number of screws they have. A twin screw extruder involves two parallel screws revolving inside the barrel. Based on the direction of the rotation of the screw, twin screw extruder is categorized into co-rotating and counter-rotating. In the co-revolving screw arrangement, both screws revolve in the same direction and in the counter-rotating screw arrangement, both screws have rotation in the opposite course. Based on the interpenetration between the screw flight and channel of both screws, a twin-screw extruder can be interpenetrated or non-interpenetrated. It is known to be an interpenetrated twin-screw system, when the flight of one screw penetrates into the passage of the remaining one. [50, 52]

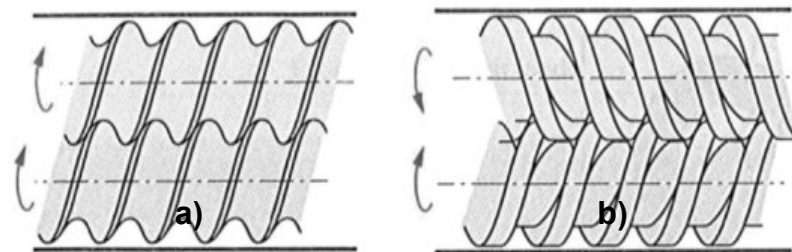


Figure 13. a) Co-rotating & b) Counter-rotating Screw System [52].

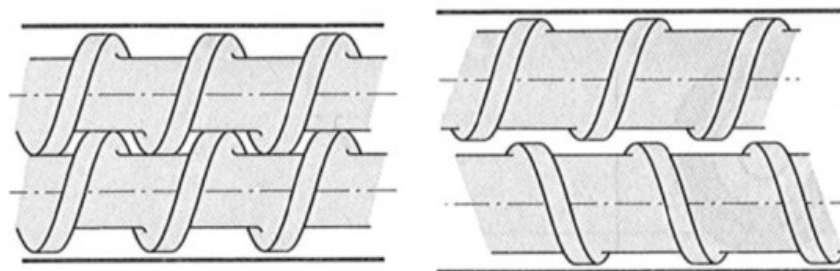


Figure 14. Interpenetrated (left) and Non-interpenetrated (right) Screw System [52].

Twin screw extruder are vastly used in the polymer industry to process and produce different polymer blends and polymer composites with pre-grinding, manual mixing and curating the polymers and reinforcements [49].

4.2 Melt Extrusion of CA/GO Bionanocomposites

Melt processing of bionanocomposites is one of the most significant processing methods since high volume of materials can be processed. Since, it is an inexpensive and quick processing method, large variety of bionanocomposites are processed. In case of processing CA/GO bionanocomposites, batch or continuous method is used. In batch processing method, micro-compounders are used in which small volume of materials are added into the feed hopper. Afterwards, melting and mixing occurs in the processing chamber. On the other hand, continuous method refers to the feeding of materials into the processing chamber constantly. According to Oksman et al. (2016), several researches have been carried out to produce cellulose based bionanocomposites on a small scale by using micro-compounder. [54] Bendaoud and Chalamet (2014), conducted the melt processing of CA polymer treated with plasticizer in a micro-twin screw extruder. According to their research, micro compounders did not allow the processing of more than 7 gm of CA powder mixed with plasticizer. They also stated that the whole processing time including the feeding time of the CA polymer samples in the batch extruder took around 5 minutes. [55] The total procedure for processing the CA/GO samples has been explained in the next chapter.

5 MATERIALS AND EXPERIMENTAL PROCEDURES

This chapter demonstrates three important issues carried out in the thesis. A complete information about 1) all the materials used during the laboratory work, 2) all the processing machines, their operating system and list of operating parameters and 3) thorough description about all the characterization of materials methods used in the thesis.

5.1 Materials

Table 2 tabulates the chemicals used in the experimental process.

Table 2. *Materials used for all the processes and the manufacturing companies.*

| No. of Ingredients | Name of the Ingredients | Manufacturing Company |
|--------------------|--|--------------------------|
| 1 | Cellulose Acetate powder | Sigma Aldrich, Germany |
| 2 | Triethyl citrate | Aldrich, Germany |
| 3 | Graphite powder | TIMCAL Ltd., Switzerland |
| 4 | Sulfuric Acid (H ₂ SO ₄) | VWR Int. OY, Finland |
| 5 | Sodium Nitrate (NaNO ₃) | Sigma Aldrich, Germany |
| 7 | Potassium Permanganate (KMnO ₄) | Merk, Germany |
| 8 | Hydrogen Peroxide (H ₂ O ₂) | Sigma Aldrich, Germany |

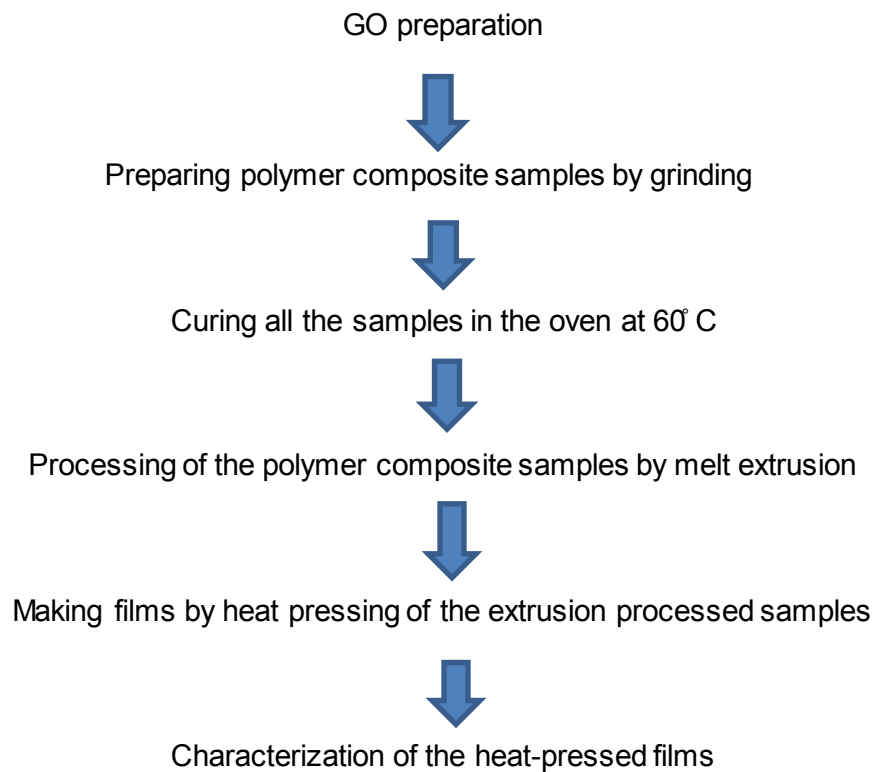
Distilled water and acetone were used for cleansing in the experimental section of the lab. GO synthesis step and manual grinding of plasticized CA polymer and composites with GO particles required the use of specific chemicals. This is properly illustrated in the Table 3.

Table 3. Chemical ingredients used in specific experimental steps.

| Experimental Step | Chemicals Used |
|--|---|
| GO preparation by modified Hummers method | Graphite powder, Sulfuric Acid (H ₂ SO ₄), Potassium Permanganate (KMnO ₄), Sodium Nitrate (NaNO ₃), and Hydrogen Peroxide (H ₂ O ₂). |
| Preparing batches of polymer composites | CA powder, TEC and Prepared GO sheets. |
| Processing of Polymer Composites | CA powder, TEC and GO. |

5.2 Process Flow of the Experimental Work

The process flow chart of the complete experimental process can be illustrated by Figure 15.

**Figure 15.** Process Flow of the Experimental Work.

5.3 Synthesis of GO by Modified Hummers Procedure

GO was produced by oxidizing graphite by following the modified Hummers procedure. The whole process can be shown in the following process flow chart.

- An ice bath was prepared.
- 46 ml of strong sulphuric acid (H_2SO_4) was transferred into a volumetric flask and the acid was placed at the ice bath at $0\text{ }^\circ\text{C}$ to make it cool. A magnetic bar stir was used for constant stirring. 0.1 gm of sodium nitrate (NaNO_3) was mixed to the cooled acid with continuous agitation.
- Graphite powder with an amount of 2 gm was added to the reaction fusion gradually with relentless stirring.
- Gradual addition of potassium permanganate (KMnO_4) with an amount of 6 gm into the reaction mixture was performed and the temperature was maintained in between $0\text{ }^\circ - 5\text{ }^\circ\text{C}$ during this period.
- Removal of ice bath was done and the reaction mix was cooled at $25\text{ }^\circ\text{C}$ for about 6 hours to result in a thick paste like substance.
- The addition of 92 ml (double the amount of acid) of distilled H_2O to the reaction mix with continuous stirring was done. The addition of distilled water results in an increase in the temperature of the reaction mixture up to around $85\text{ to }90\text{ }^\circ\text{C}$.
- After half an hour of continuous stirring, addition of 280 ml of distilled water to the reaction mix was done.
- The addition of 3 ml of 30% H_2O_2 was done to the reaction solution, which results in a change in hue of the mixture to yellow from dark brown.
- The obtained product was centrifuged and the remaining bottom fraction was collected. The obtained bottom portion was again dispersed in distilled water and centrifuging was performed few times till the pH of the solution gets to seven. Ultra sonication were being done frequently in between centrifuging.
- When the mixture gets to neutral, it was taken in petri dishes and the material was cured in the oven for about 12 hours at around $55\text{ }^\circ\text{C}$.
- The dried GO films for the petri dishes were collected by using a sharp knife. The pictures of the centrifuged mixtures and the GO films are illustrated in Figure 16.

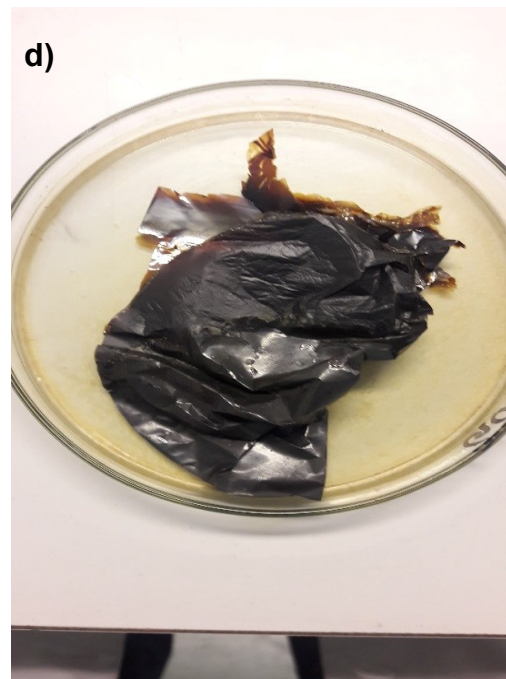
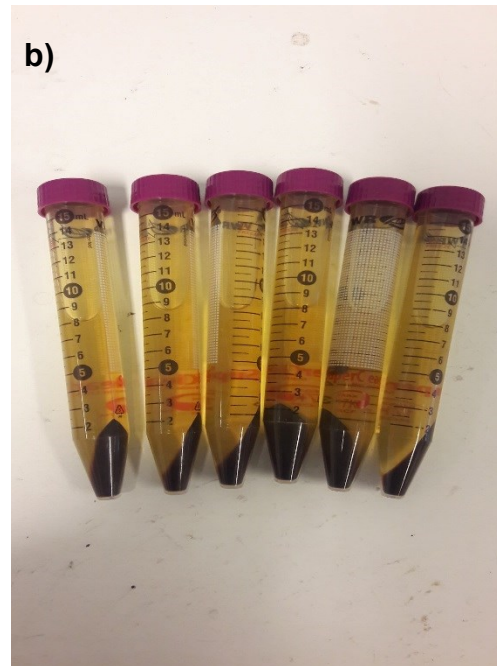


Figure 16. Pictures Taken during GO Synthesis- a) Compactor, b) Centrifuged GO Solutions, c) Sonicator, d) Dried GO Film.

5.4 Manual Grinding and Mixing of the Samples

Two sets of four samples were prepared by manual grinding using mortar and pestle. CA powder was mixed with TEC plasticizer to make the first pure polymer sample. Second, third and fourth sample were made with mixing finely grinded GO with the plasticizer and CA powder. In the second, third and fourth polymer composite samples, the ratio of GO was 0.25, 0.5 and 0.65 wt.% consecutively with respect to the amount of CA. Ratio of the plasticizer on the weight of CA was kept constant in all the samples. Table 4 illustrates the recipe for making the polymer and composite samples with manual mixing.

Table 4. Recipe for making manually grinded polymer and composite samples.

| Sample No. | Materials and Used Amount |
|------------|---|
| 1. | Cellulose acetate = 3 gm + Triethyl citrate- 50 wt. % w.r.t. CA = 1.5 gm |
| 2. | Cellulose acetate = 3 gm + Triethyl citrate- 50 wt. % w.r.t. CA = 1.5 gm + GO- 0.25 wt. % w.r.t. CA = 7.5 mg |
| 3. | Cellulose acetate = 3 gm + Triethyl citrate- 50 wt. % w.r.t. CA = 1.5 gm + GO- 0.5 wt. % w.r.t. CA = 15 mg |
| 4. | Cellulose acetate = 3 gm + Triethyl citrate- 50 wt. % w.r.t. CA = 1.5 gm + GO- 0.65 wt. % w.r.t. CA = 19.5 mg |

5.4.1 Procedure for Sample Preparation

For preparing the pure polymer sample, 3 gm CA was weighed and kept in a plastic container. An approximate one-third portion of the 3 gm CA was taken in the mortar and one-third of the 1.5 gm plasticizer was added to the mortar by using a dropper. The material was blended properly using a pestle. When it got properly mixed, rest of the CA was mixed with the rest of the plasticizer in two segments using the same way. The prepared plasticized CA sample was preserved in a covered container.

For preparing the second, third and fourth polymer composite samples with pre-calculated amount of GO, same procedure was performed. 3 gm of CA powder was weighed and kept in a plastic container. Pre-calculated amount of finely grinded GO was also weighed and taken in the mortar. Few drops of the 1.5 gm plasticizer were added to the mortar and grinded well to make the GO particles as dispersed as possible. Small portion of the 3 gm CA powder was added to the mortar and mixed well with the pestle. The rest

of the CA was mixed with the rest of the plasticizer in two segments using the same way. In second, third and fourth sample, the ratio of GO used was 0.25, 0.5 and 0.65 wt.% consecutively with respect to the amount of CA, but the same procedure was followed for preparing the polymer composite samples. Figure 17 and 18 illustrates the prepared TEC plasticized CA and CA/GO composite samples.



Figure 17. Pure CA Sample Mixed with TEC.

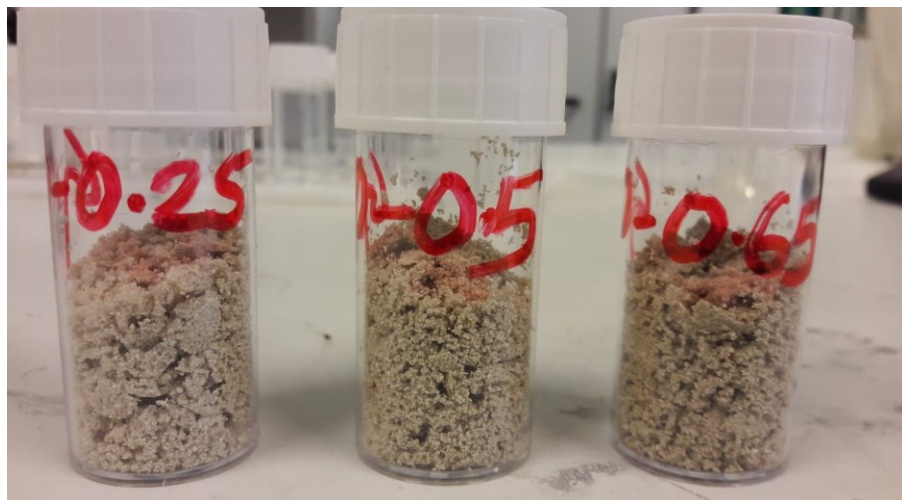


Figure 18. Manually Mixed GO 0.25, GO 0.50 and GO 0.65 Composite Samples.

5.5 Processing of the Samples

The TEC plasticized CA and the composite samples with varying ratio of GO were processed by DSM Xplore 5, twin screw micro-compounder in the laboratory of Tampere University (TUNI). This twin screw extruder is a 2005 model having a capacity of 5 cm³. The screws are co-rotating having a length 90 mm each. The machine can process maximum at 400 °C. The machine includes six heating zones with three front and three rear zones that can be controlled by a touch screen monitor. This twin screw extruder has the benefit to process polymer batches of very small weight. Figure 19 illustrates the twin screw extruder setup in TUNI.



Figure 19. Twin-Screw Extruder in Laboratory.

5.5.1 Processing Procedure and Operating Parameter

Since CA has high moisture absorbency, drying of all the samples was performed in the oven for few hours at around 55 °C just prior to the processing. Before processing of the samples, the extruder was cleaned by feeding the cleaning polymer at 200 °C. The plasticized CA sample and the CA/GO (varying ratio of GO) composite samples mixed with TEC were all processed at 200 °C for about 3 minutes. The speed of the screw was kept at 80 rpm for all the samples. The plasticized CA sample was transparent when processed and all the other CA/GO composite samples were increasingly darker in color after processing. All the four samples were processed in one run. A temperature range of 170 °C to 200 °C was trialed to process the samples, but processing at 200 °C gave the best processed the samples. One extra batch of samples were prepared in the similar way for the analysis and safety purpose. After each use of the extruder, it was cleaned by the cleaning polymer. The processed samples are illustrated in the Figure 20.



Figure 20. Processed Samples- TEC plasticized a) CA, b) GO 0.25, c) GO 0.50 and d) GO 0.65 Composite samples.

5.6 Heat Pressing the Samples

After processing the samples in the extruder, they were pressed by the heat presser to yield a film formation. Before the heat pressing of the samples, they were cut into small pieces for the pressing convenience. The hydraulic pressing machine used during the film formation has two parallel plates. The temperature of both the upper and the lower heating plates can be controlled individually. Baking paper was placed on the lower heating plate and above it; the small cut pieces of the samples were placed. Another piece of baking paper was placed above the cut pieces of sample. Baking paper was used to resist sticking of the polymer samples to the heating plates. Since all the samples were processed at 200 °C, same temperature was used to press all the samples. The pressure of the heat press was kept at 6 bar. All the four samples were pressed for 20 seconds. The hydraulic press setup in the laboratory is illustrated in Figure 21.



Figure 21. Heat Pressing Machine Setup.

The pressed samples were preserved in transparent zip-lock plastic bag for further analysis. The pressed film samples are illustrated in Figure 22.

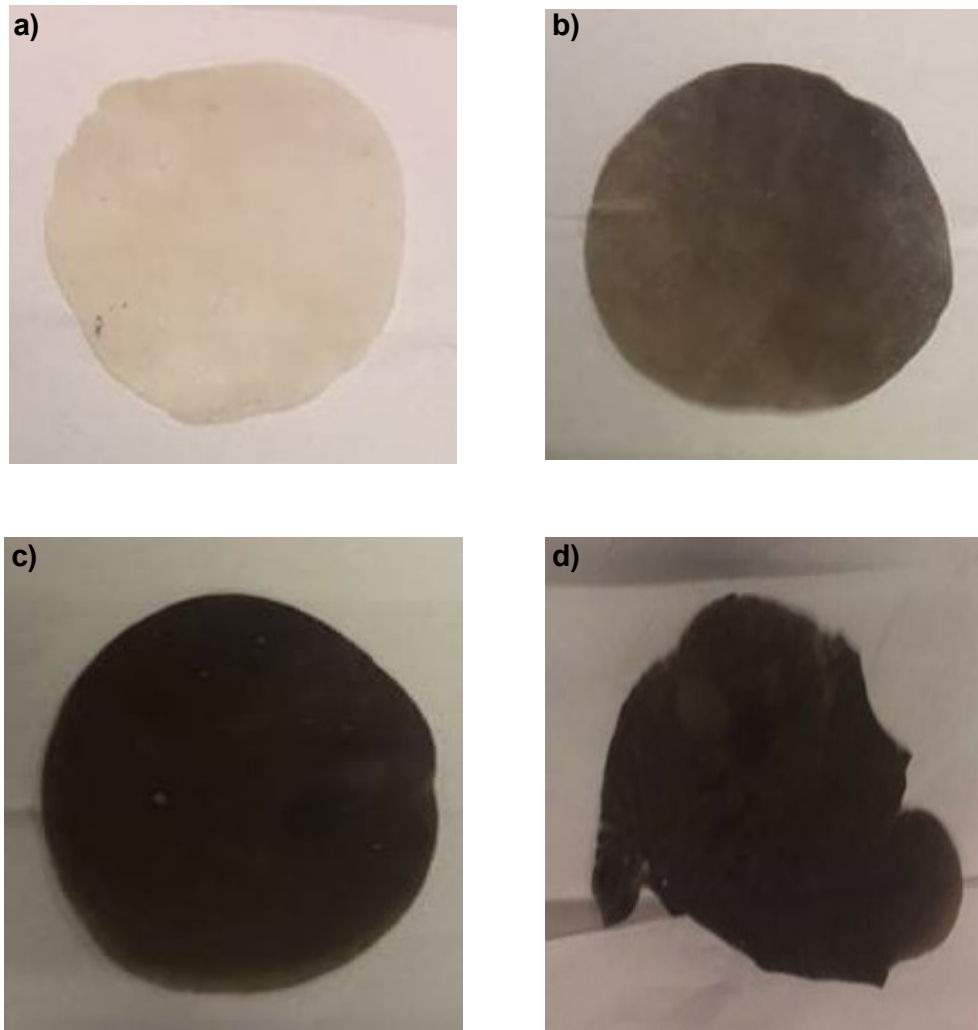


Figure 22. Heat-pressed TEC plasticized Polymer and Composite Samples- a) CA, b) GO 0.25, c) GO 0.50 and d) GO 0.65

6 CHARACTERIZATION OF MATERIALS

Various methods were performed for the characterization of the fabricated TEC plasticized CA and CA/GO composite films. All the data-based and quality-based information obtained from the characterization methods were used to compare TEC plasticized CA film with the TEC plasticized CA/GO composite samples as well as the comparison within the composite samples with varying percentage of GO was also analyzed. The characterization methods used to analyze the samples were- Fourier Transform Infrared Spectroscopy (FTIR), Wide Angle X-Ray Scattering (WAXS), Thermogravimetric Analysis (TGA), Differential Scanning Calorimetry (DSC), Field Emission Scanning Electron Microscopy (FESEM) and Mechanical properties.

6.1 Fourier Transform Infrared Spectroscopy (FTIR)

Chemical arrangement and interaction among the functional groups of the polymer nanocomposite material can be straightly achieved from the FTIR spectroscopy. The data measurement from the from the FTIR spectra is very reliable and precise. This method is acknowledged for the industrial and research facilities. [56]

In the FTIR spectroscopy, the radiation transmittance (%) of the samples was obtained as a function of the wavenumber which is inverse to the wavelength of the radiation. The characteristic peaks achieved because of the interaction of different functional groups in the samples were analyzed. For analyzing the interaction between CA and GO, the FTIR spectra of the TEC plasticized CA film and the CA/GO composite films were taken. There are different oxygen based functional groups prominent in the GO film. Different characteristic peaks in the spectra of GO can be visible because of the existence of different oxygen comprising functional groups in GO film. Bruker Optics Tension 27 was used for the FTIR measurements. The measurement of spectra was done at a range between 500 cm^{-1} and 4000 cm^{-1} .

6.2 Wide Angle X-Ray Scattering (WAXS)

Polymer characterization based on diffraction can be performed with X-rays having wavelength between 0.1 and 2.5 Å. The wavelength of X-rays allows obtaining the diffraction measurements that make it possible to analyze structures at sub nanometer to sub micrometer length scales. X-rays interact with the crystalline portion of the polymer

or polymer composite in X-ray diffraction. This interaction causes a diffraction pattern. [57]

In this thesis work, the WAXS measurements of the GO film, TEC plasticized CA polymer film and CA/GO composite films were performed by means of Panalytical Empyrean Multipurpose Diffractometer. 40 KV and 40 mA were the operating parameters for this instrument as well as the used radiation source was $K\alpha$ ($\lambda=0.154\text{nm}$). The WAXS data was recorded from $2\theta = 5^\circ$ to 40° . The scan rate was 2° per minute. An amorphous sample holder was used to attach the GO, pure CA and CA-GO composite samples.

6.3 Differential Scanning Calorimetry (DSC)

Thermal analysis performed with DSC is a vastly used method. The amount of heat absorbed in relative to a reference can be determined through a particular thermal shift by this thermal analysis method. The thermal properties of the sample going through considerable change can be estimated with respect to time or a fixed heating or cooling proportion as a function of temperature. [58]

A temperature window of 0°C to 200°C was used for the measurements of Differential Scanning Calorimetry. The rate of heating was $10^\circ\text{C} / \text{minute}$. The instrument used was NETZSCH DSC 214 Polyma. The measurements were performed in a nitrogen atmosphere. The glass transition temperature of the TEC plasticized CA and CA/GO composite samples were obtained by the DSC thermo-grams. 10 mg of material from the composite films were weighed in the aluminum pans and sealed with a universal crimper.

6.4 Thermogravimetric Analysis (TGA)

In this technique, the alteration in the sample mass is observed as a function of time and temperature. The method is executed with a thermal-balance. TGA can be dynamic and isothermal. TGA method is renowned to analyze the thermal stability of polymer or polymer composite materials at various applying environments. [59]

In the laboratory, the thermal property of TEC plasticized CA and CA/GO composite samples were analyzed by NETZSCH TG209 F3. In this research, isothermal TGA method was used. 10 mg of samples from the each of the films were kept at 200°C for about 3 minutes which are also equal to the processing time and temperature of the samples. After spending 3 minutes at 200°C , the loss of mass were estimated from the TGA curves for the TEC plasticized CA and the CA/GO composite films. The process was conducted in a nitrogen atmosphere.

6.5 Field Emission Scanning Electron Microscopy (FESEM)

FESEM is a type of scanning electron microscopy based diagnostic strategy where the electrons are released from a field emission gun. This technique is well used to analyze the morphological structure of polymers and composites. [60]

Using a field emission microscope helped investigate the cross-sectional morphological structure of CA/GO composite films. The brand name of the microscope is SEM Zeiss ULTRA Plus. The composite films cut into required size, were plummeted into liquid nitrogen and frozen fractured. Gold coating was done to the fractured surface before the investigation of the morphology by microscope to resist charging.

6.6 Mechanical Testing

The mechanical properties of the TEC plasticized CA and the CA/GO composite films were investigated by performing mechanical testing. The films having regular thickness were exposed to tensile testing by means of a universal testing machine (Instron 5967). The strain rate was 2mm/min at 20 °C. The TEC plasticized CA and CA/GO composite samples were cut into a specific dumbbell shape having a dimension of 12 mm × 2 mm × 0.1 mm. Five samples were prepared from each film which gave five corresponding values to calculate statistical average of the mechanical parameters.

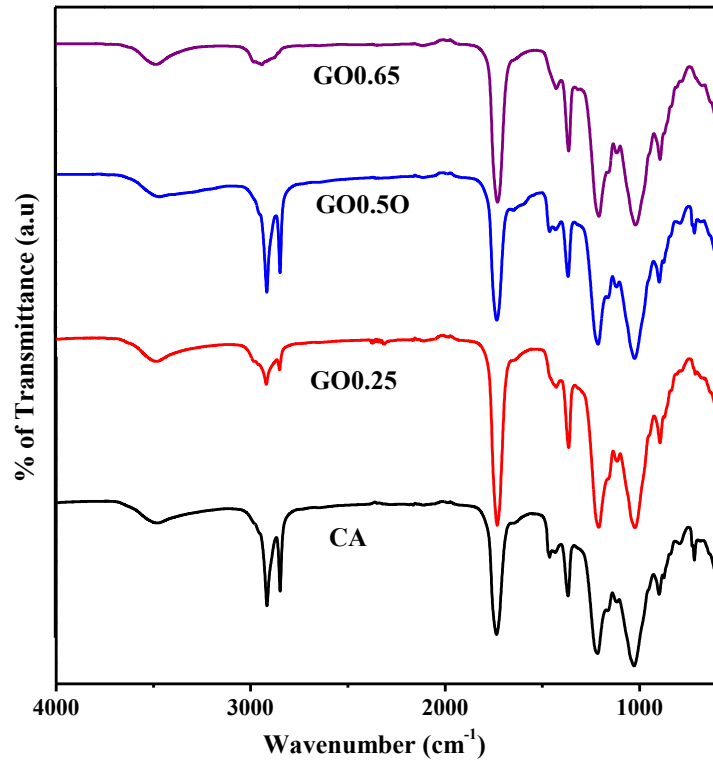
7 RESULTS AND DISCUSSION

All the values, graphs and data obtained from the characterization methods are presented and analyzed in this section of the thesis. The comparison between the TEC plasticized CA and the CA/GO composites having different GO concentration are analyzed in this section. The reasons for the changes in results in the characterization methods because of the addition of GO in the CA polymer matrix have been discussed thoroughly. The changes in the results due to the growth in the concentration of GO in the CA/GO polymer composites have been taken under focus too in this section.

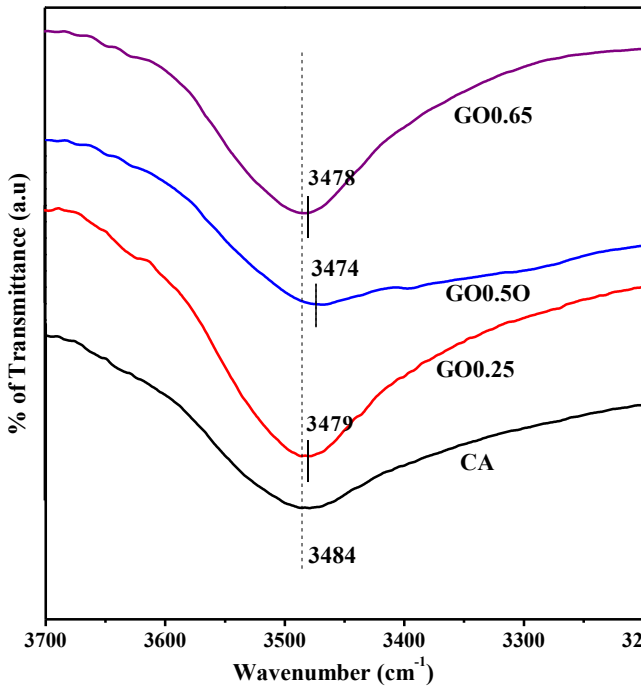
7.1 FTIR Results

In the Figure 23 (a), the FTIR spectra of TEC plasticized CA and CA/GO composite films are presented. TEC plasticized CA demonstrates characteristic broad peak at around 3484 cm^{-1} because of the O-H stretching vibration of hydroxyl groups. C-O-C stretching vibration at 1736 cm^{-1} occurs due to the glucoside units in the cellulose backbone. [61] However, the interaction between GO and CA is confirmed by the shifting of the FTIR peaks position of the -OH stretching vibration peak and C-O-C stretching vibration peak in the composite films from the TEC plasticized CA film [62, 63].

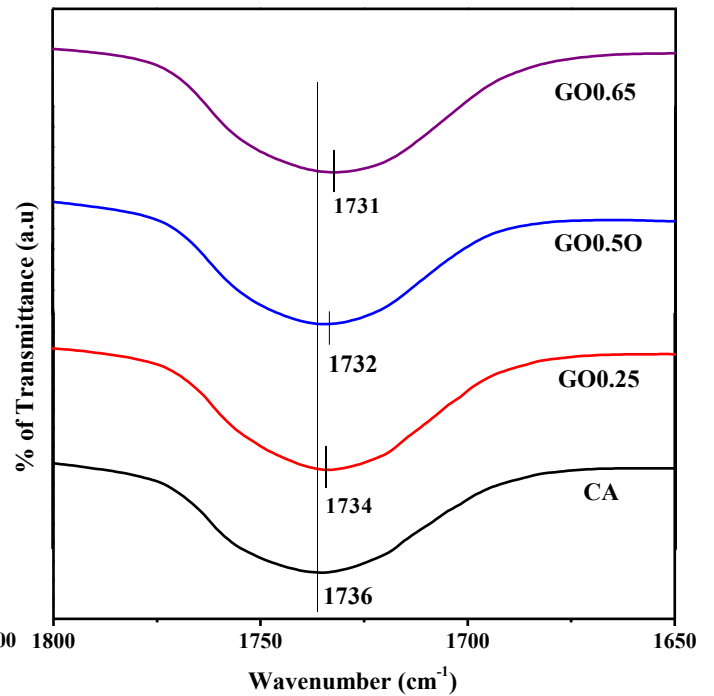
The Figure 23 (b) is an enlarged version of the -OH stretching vibration region for the TEC plasticized CA and the CA/GO composite films. In this figure, it is noticeable that the -OH stretching peak of the composite films have shifted to some extent as compared to the -OH stretching peak of TEC plasticized CA. In the spectra of GO 0.25, GO 0.50 and GO 0.65 composite films, the -OH stretching peak occurs at 3479 cm^{-1} , 3474 cm^{-1} and 3478 cm^{-1} respectively which are lower in terms of wavenumber when compared to the -OH stretching peak of TEC plasticized CA. Hence, in the FTIR spectra of CA/GO composite films, the -OH stretching peaks shift to a lower wavenumber with the increase of the GO content in the nanocomposite films. This is an indication of the hydrogen bonding interaction occurring between TEC plasticized CA and GO. [62, 63]



a)



b)



c)

Figure 23. a) FTIR Spectra of a) Plasticized CA and CA/GO Composite Films, b) Zoomed O-H Stretching band and c) Zoomed C-O-C Stretching Band

The Figure 23 (c) is an enlarged version of the C-O-C stretching vibration region for the TEC plasticized CA and the CA/GO composite films. In the FTIR spectra of plasticized CA, the C-O-C stretching vibration occurs at 1736 cm^{-1} . However, in the spectra of GO 0.25, GO 0.50 and GO 0.65 composite films, the C-O-C stretching peaks shift to 1734 cm^{-1} , 1732 cm^{-1} and 1731 cm^{-1} respectively which are lower in terms of wavenumber when compared to the C-O-C stretching peak of TEC plasticized CA. These shifts of the C-O-C stretching peaks in the composite films also give the indication of hydrogen bonding interaction among the GO sheets and the CA matrix. [63]

7.2 WAXS Results

The dispersion of GO nano sheets into the CA polymer matrix of the CA/GO composite films are analyzed and the interlayer spacing between GO layers are calculated from Bragg's law [13]. The WAXS patterns of GO, TEC plasticized CA and CA/GO composite films are illustrated in Figure 24. A typical diffraction peak of GO appears at $2\theta=10.8^\circ$ signifying the interlayer distance of 0.82 nm, which is caused by the oxygen containing groups at the edges of the GO sheets and the trapped H_2O molecules in between GO sheets [64, 65].

TEC plasticized CA shows characteristic broad diffraction peak at $2\theta=8.7^\circ$ and $2\theta=21.74^\circ$ both due to the amorphous part of the polymer [13, 21]. The CA/GO composite films show similar diffraction peaks compared to the TEC plasticized CA film. There is no observation of the characteristic peak of GO in the CA/GO composite films and this is due to the disorder and lack of structure uniformity in GO. It also signifies good dispersion of the GO sheets at molecular level into the TEC plasticized CA polymer matrix. [66] The d spacing of GO sheets before compounding can be estimated by the following formula from Bragg's law-

Pure GO before Compounding:

$$d = \lambda / 2 \sin \theta = 0.154\text{ nm} / 2 \sin (10.8^\circ) = 0.82\text{ nm}$$

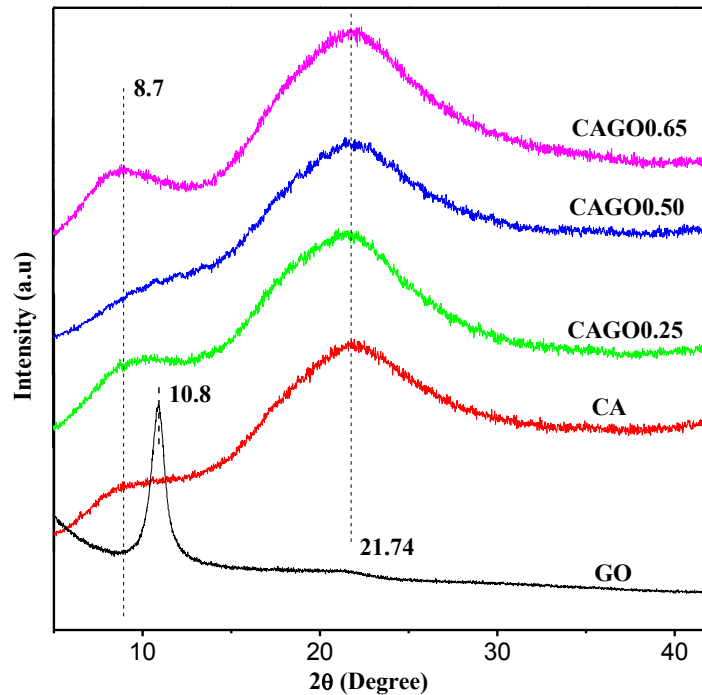


Figure 24. WAXS of GO, TEC Plasticized CA & CA/GO Composite films.

7.3 DSC Results

Thermograms obtained from DSC studies show the thermal characteristics of TEC plasticized CA and CA/GO composite films. DSC thermogram in the Figure 25 shows the T_g of the TEC plasticized CA polymer film and the CA/GO composite films. The temperature region from 98 °C TO 103 °C in the DSC thermograms corresponds to the T_g of the TEC plasticized CA and the CA/GO composite films. The CA film processed with TEC plasticizer demonstrates a broad endothermic peak positioned at 98 °C. Derivatives of cellulose demonstrate this kind of ideal endothermic peak in the DSC thermogram at a higher temperature. [21] With the treatment of TEC, the softening temperature of CA gets reduced to 98 °C which is almost half of the T_g of unplasticized CA film, recorded by Bao et al. (2015) in their research. The t_g of Unplasticized CA was recorded at around 192 °C, according to Bao et al. (2015). [12] It is noticeable from Figure 25 and Table 5 that, the increase in the GO concentration in the CA/GO composite films is causing a substantial increase of the T_g of the composite films as compared to the T_g of TEC plasticized CA film. The GO 0.5 composite film shows a maximum increase in the T_g which is 103 °C. T_g of GO 0.25 and GO 0.65 composite films are 102 °C & 101 °C respectively. The hydrogen bonding interaction between the CA and GO sheets is the reason for the

softening of CA/GO composite films at higher temperatures as compared to the TEC plasticized CA polymer film. The segmental movement of the CA polymer chain is reduced because of the interaction between CA polymer matrix and GO sheets that causes an increase of T_g in the composite films compared to TEC plasticized CA film. [21] DSC thermograms of TEC plasticized CA and different CA/GO composites are illustrated in the Figure 25 and Table 5.

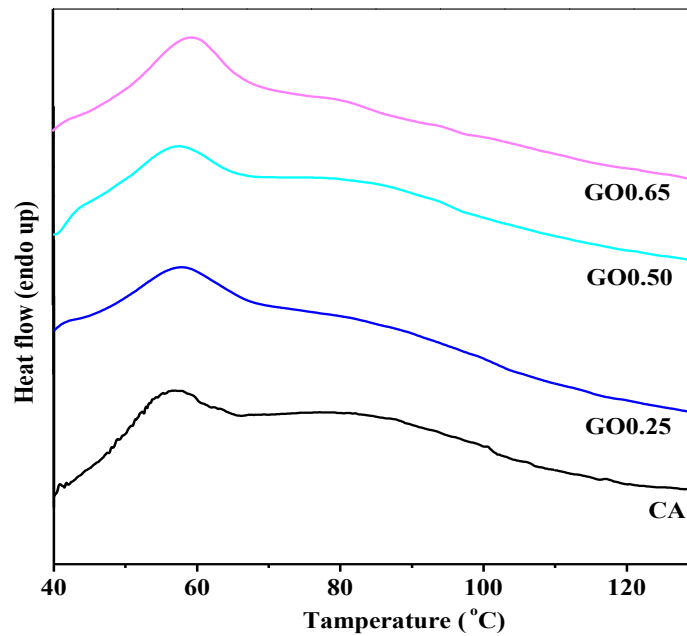


Figure 25. DSC Thermograms of TEC plasticized CA and CA/GO Composite Films.

Table 5. T_g of TEC plasticized CA and CA/GO composite films from DSC thermograms.

| Samples | T_g |
|----------------|--------|
| Plasticized CA | 98 °C |
| GO 0.25 | 102 °C |
| GO 0.50 | 103 °C |
| GO 0.65 | 101 °C |

7.4 TGA Results

Isothermal TGA was performed to analyze the mass loss (%) due to the evaporation of plasticizer from the TEC plasticized CA and CA/GO composites based on time and temperature. Since the temperature and time needed for melt processing of all the samples were 200 °C and 3 minutes respectively, they were kept at the same temperature as well as same time period was used to monitor the mass loss (%) from the samples due to the evaporation of TEC. Mass loss (%) of TEC plasticized CA and CA/GO composite samples can be analyzed from the thermograms obtained in the Figure 26.

By the TGA curve of TEC plasticized CA, it is noticeable that TEC plasticized CA has 93.2 % residual mass after 3 minutes at 200°C which means it loses 6.8 % of the initial weight. In the TGA curve of TEC plasticized GO 0.65 composite film, the mass reduced is found to be 6 % which is almost 1% less than TEC plasticized CA. TEC plasticized GO 0.5 and GO 0.25 composite films show mass loss of 6.8 % and 7.2 % respectively. Therefore, all the composite films show better or almost similar residual mass as compared to the TEC plasticized CA polymer film. Thus, TEC plasticized CA/GO composite samples show decent thermal property as compared to the TEC plasticized CA polymer film. This happens because of the interaction of the functional groups between GO and CA through hydrogen bonding. [13]

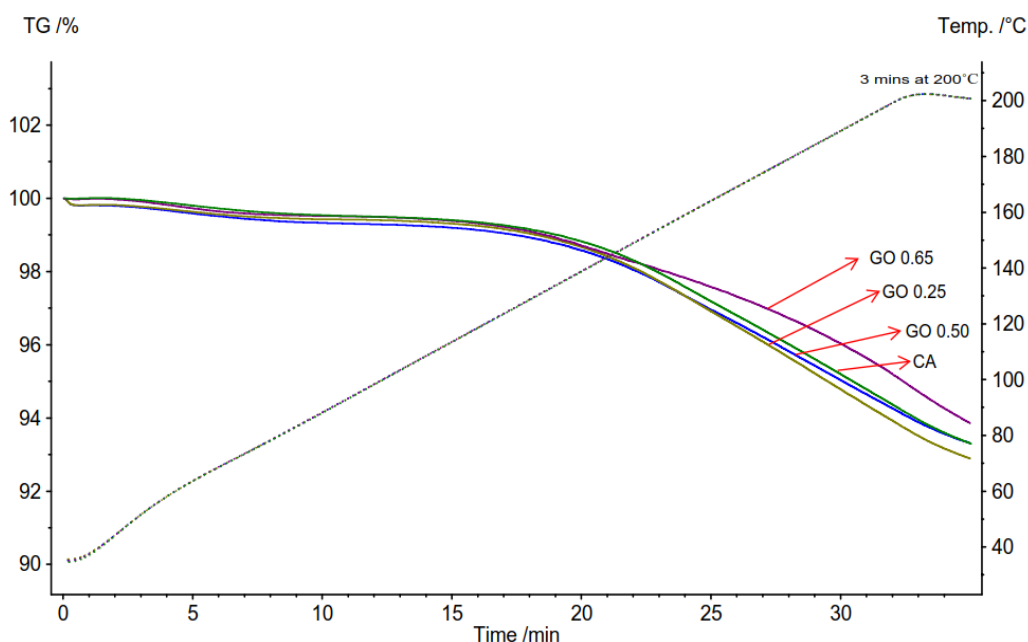


Figure 26. Isothermal TGA Curves for TEC Plasticized CA and CA/GO Composite films.

7.5 FESEM Images

The morphology of TEC plasticized CA and the CA/GO composite films were examined by FESEM studies and resulted SEM images are presented in Figure 27. These FESEM images also demonstrate the dispersed GO sheets into the CA polymer matrix. Any possible agglomeration of GO sheets into the polymer matrix can be easily noticeable by these FESEM images. Figure 27 demonstrates normal and magnified FESEM images of the TEC plasticized CA and CA/GO composite films.

The fractured surface of TEC plasticized CA film, independent of GO particles exhibits a smooth and clean cross-sectional FESEM images. On the other hand, the FESEM images of the fractured surfaces of the GO 0.25 and GO 0.5 composite films demonstrate uniformly dispersed of GO sheets into the CA matrix. In the FESEM images of these two CA/GO composite films, the GO sheets seem to be well dispersed into the CA matrix because of the generation of shear stress at the period of melt processing. However, as the concentration of GO sheets increase up to 0.65% in the CA/GO composite film, the agglomeration of GO sheets becomes very prominent. Hence, the GO sheets get clustered into the CA polymer matrix. In the GO 0.65 composite film, the amount of GO content increases to a certain point which makes the GO sheets very close to each other. As a result of that, the GO sheets become stacked into the CA polymer matrix. [13] Furthermore, at higher GO concentration, the sheets of GO tend to aggregate in the polymer matrix owing to the presence of strong Van Der Waals (VDW) bonding within the GO sheets [21, 67].

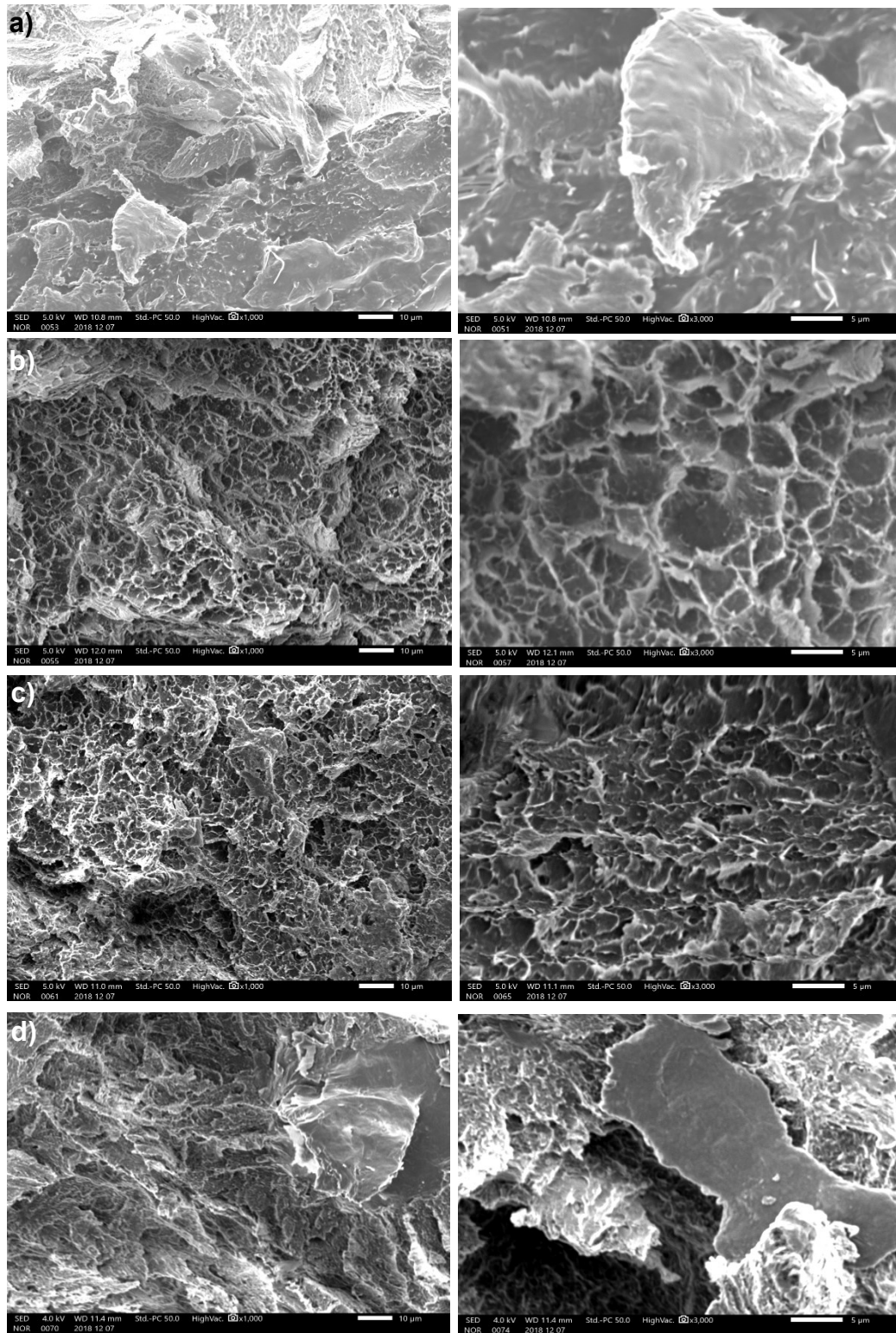


Figure 27. FESEM Images of TEC Plasticized a) CA, b) GO 0.25, c) GO 0.5 and d) GO 0.65 Samples

7.6 Mechanical Properties

The ideal stress-strain curves obtained from the mechanical testing experiment of the TEC plasticized CA and CA/GO composite films are presented in the Figure 28. Five analogous data of stress at break, strain at break and Young's modulus were obtained by repeating each measurement for five times. By using these different values, statistical average of the above mentioned properties were calculated. The calculated statistical average values for TEC plasticized CA and CA/GO composite films are presented in Table 6.

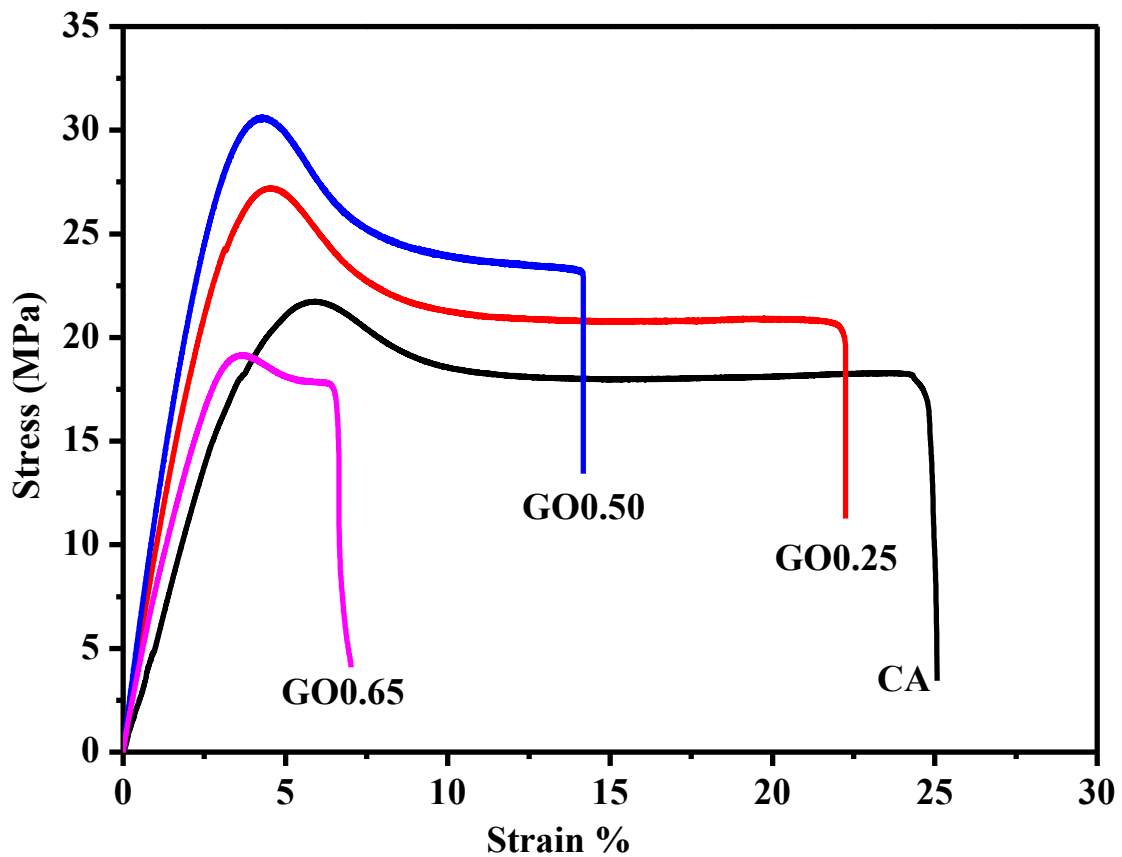


Figure 28. Stress-Strain Curves for TEC Plasticized CA and CA/GO Composite Films.

From the Figure 28 and Table 6, it is very noticeable that, the stress at break increased whereas the elongation at break decreased of the TEC plasticized CA/GO composite films with the increase of GO content as compared to the TEC plasticized CA film. The elongation at break for the TEC plasticized CA film is found to be 26 ± 4 %. On the other hand, GO 0.50 composite film shows a strain at break of 15 ± 3 % which is much lower than the TEC plasticized CA film. Reduction of the elongation at break of the composite

films with higher GO content in the polymer matrix refers to the lowering of ductility of composite films. TEC plasticized CA film shows a stress at break of 16 ± 4 MPa. On the other hand, GO 0.25 and GO 0.50 composite films show uniformly increased stress at break of 20 ± 3 and 25 ± 4 MPa respectively. [21] However, the TEC plasticized GO 0.65 composite produce very brittle film and it exhibits both lower stress at break (15 ± 2 MPa) and strain at break (5 ± 2 %) compared to the TEC plasticized CA film. The strong VDW interaction between the GO sheets in TEC plasticized CA matrix at higher GO concentration leads to the agglomeration of the GO sheets into the CA matrix which makes the GO 0.65 film brittle [21, 67]. The Young's modulus of the composite films also enhances with the enhancement of the GO content in the TEC plasticized CA matrix except the TEC plasticized GO 0.65 film. TEC plasticized GO 0.25 (0.70 ± 0.4 GPa) and GO 0.5 (1.1 ± 0.6 GPa) composite films show significantly higher values of Young's modulus compared to that of the TEC plasticized CA film (0.50 ± 0.3 GPa). The clustering of GO sheets into the TEC plasticized CA matrix at higher GO concentration causes the reduced Young's modulus value in case of GO 0.65 composite film. [21]

In conclusion, GO 0.25 composite film shows 25 % and 40 % improvement of stress at break and Young's modulus respectively as compared to TEC plasticized CA, whereas GO 0.50 composite film demonstrates 56 % and 120 % increase of stress at break and Young's modulus respectively. Mechanical testing of the samples shows significant expansion of tensile strength of the composite films with higher GO content and this is due to the strong interaction between the TEC plasticized CA and the GO sheets via the formation of hydrogen bond [68].

Table 6. Mechanical properties of TEC plasticized CA and CA/GO composite films with statistical avg.

| Sample | Stress at Break (MPa) | Strain at Break (%) | Young's modulus (GPa) |
|---------|-----------------------|---------------------|-----------------------|
| CA | 16 ± 4 | 26 ± 4 | 0.5 ± 0.3 |
| GO 0.25 | 20 ± 3 | 22 ± 3 | 0.7 ± 0.4 |
| GO 0.50 | 25 ± 4 | 15 ± 3 | 1.1 ± 0.6 |
| GO 0.65 | 15 ± 2 | 5 ± 2 | 0.6 ± 0.3 |

8 FURTHER RESEARCH

Producing bionanocomposite films using CA as a polymer matrix and GO as reinforcement gave some good consequences. This work truly inspires to carry on performing some other researches based on the outcome. There are some other polymers that are biodegradable in nature such as poly lactic acid. Poly lactic acid can be processed by melt extrusion with GO as a reinforcement to produce strong bionanocomposite film. The focus should be on producing bio-based nanocomposites which will be eco-friendly. Reduced graphene oxide which is very close to pristine graphene can also be used to observe the mechanical effect of the processed composite film.

Focus should be on producing biodegradable composite films having good mechanical properties to use in packaging applications for food and other products. Further analysis can be performed on the estimation and experimentation of the gas barrier properties of the bionanocomposite films.

CONCLUSIONS

In this thesis work, biodegradable cellulose acetate (CA) polymer was processed with very low content of graphene oxide (GO) nano sheets in order to fabricate bionanocomposite films. The main focus of this research work was to perform the processing of CA/GO biocomposite samples by melt extrusion which is suitable for large scale production in the industries. Furthermore, the possibility to fabricate mechanically strong CA/GO composite films was a significant intention to conduct this thesis work since bio based polymers have lower mechanical strength as compared to petroleum based plastics.

Structural and thermal characterization as well as mechanical testing methods have been used to analyze the performance of the TEC plasticized CA/GO composite films with respect to TEC plasticized CA film. The hydrogen bonding interaction between the CA matrix and GO sheets has been confirmed from the FTIR spectra. Presence of GO sheets in the composite films has been ensured since the characterization peaks in the TEC plasticized CA/GO composite films shifted to some extent as compared to the peaks of TEC plasticized CA film. The WAXS study and FESEM images backs the integration and dispersion of GO into the CA polymer matrix in both GO 0.25 and GO 0.50 composite films. However, GO 0.65 composite film demonstrates clustered GO sheets into the CA matrix. CA/GO composite films illustrate good thermal property and it has been confirmed through DSC and isothermal TGA analysis. Higher T_g has been obtained from the DSC curves for the TEC plasticized CA/GO composite films as compared to the TEC plasticized CA film which ensures the interfacial interaction among GO and CA polymer matrix. Isothermal TGA curves illustrate reduced loss of mass for the composite films at 200°C as compared to the mass loss of TEC plasticized CA. Mechanical testing shows a significant enhancement of the mechanical strength of TEC plasticized GO 0.25 and GO 0.50 composite films as compared to TEC plasticized CA film. A higher stress at break and Young's modulus is prominent for the CA/GO biocomposite films.

Green packaging is considered a very important issue in this recent time since the necessity of biodegradable packaging products has enhanced a lot in order to create an eco-friendly environment. Approaches and researches like this thesis work can definitely become successful to replace petroleum based packaging products with the biodegradable nanocomposite based products which have excellent mechanical properties. Incorporation of a very small content of GO into bio based polymer matrix can increase the

mechanical properties to great extent. It is high time, we carry out more and more researches to produce eco-friendly biodegradable composite films for the packaging applications.

REFERENCES

- [1] Zhao, R., Torley, P. & Halley, P.J. (2008). Emerging biodegradable materials: starch- and protein-based bio-nanocomposites, *Journal of Materials Science*, Vol. 43(9), pp. 3058-3071.
- [2] Ebnesajjad, S. (2012). *Handbook of Biopolymers and Biodegradable Plastics: Properties, Processing, and Applications*, Elsevier/William Andrew, Amsterdam; Boston, pp. 1.
- [3] Selke, S.E.M. & Culter, J.D. (2016). *Plastics packaging: properties, processing, applications, and regulations*, Third ed. Hanser Publishers, Munich; Cincinnati, pp. 3-5
- [4] Rosato, D.V., Rosato, M.G. & Schott, N.R. (2010). *Plastics technology handbook: Volume 1: introduction, properties, fabrication, processes*, 1st ed. Momentum Press, [New York, N.Y.], pp. 59, 60, 74.
- [5] Muralisrinivasan Subramanian, N. (2016). *Plastics waste management: processing and disposal*, Smithers Rapra, Shawbury, Shrewsbury, Shropshire, U.K, pp. 1, 2.
- [6] Goodship, V. (2007). *Introduction to plastics recycling*, 2nd ed. Smithers Rapra, Shawbury, U.K, pp. 4, 5.
- [7] Chandra, R. & Rustgi, R. (1998). Biodegradable polymers, *Progress in Polymer Science*, Vol. 23(7), pp. 1273-1335. Available: <https://www.sciencedirect.com/science/article/pii/S0079670097000397>
- [8] Siracusa, V., Rocculi, P., Romani, S. & Rosa, M.D. (2008). Biodegradable polymers for food packaging: a review, *Trends in Food Science & Technology*, Vol. 19(12), pp. 634-643. Available: <https://www.sciencedirect.com/science/article/pii/S0924224408002185>
- [9] Klemm, D., Heublein, B., Fink, H. & Bohn, A. (2005). *Cellulose: Fascinating Biopolymer and Sustainable Raw Material*, *Angewandte Chemie International Edition*, Vol. 44(22), pp. 3358-3393. Available: <https://doi.org/10.1002/anie.200460587>.

- [10] Cellulose 2018. *Britannica Academic*. Retrieved 13 November 2018, from <https://academic.eb.com/levels/collegiate/article/cellulose/22028>
- [11] Cellulose acetate 2018. *Britannica Academic*. Retrieved 13 November 2018, from <https://academic.eb.com/levels/collegiate/article/cellulose-acetate/22029#>
- [12] Bao, C.Y., Long, D.R. & Vergelati, C. (2015). Miscibility and dynamical properties of cellulose acetate/plasticizer systems, *Carbohydrate Polymers*, Vol. 116 pp. 95-102.
Available: <http://www.sciencedirect.com/science/article/pii/S0144861714007693>.
- [13] Jeon, G.W., An, J. & Jeong, Y.G. (2012). High performance cellulose acetate propionate composites reinforced with exfoliated graphene, *Composites Part B*, Vol. 43(8), pp. 3412-3418. Available: <https://www.sciencedirect.com/science/article/pii/S1359836812000297>
- [14] Quintana, R., Persenaire, O., Bonnaud, L. & Dubois, P. (2012). Recent advances in (reactive) melt processing of cellulose acetate and related biodegradable bio-compositions, *Polymer Chemistry*, Vol. 3(3), pp. 591-595.
Available: <https://pubs.rsc.org/en/content/articlehtml/2012/py/c1py00421b>
- [15] Charvet, A., Vergelati, C. & Long, D.R. (2019). Mechanical and ultimate properties of injection molded cellulose acetate/plasticizer materials, *Carbohydrate Polymers*, Vol. 204 pp. 182-189. Available (accessed ID: 271345): <http://www.sciencedirect.com/science/article/pii/S0144861718311895>.
- [16] Wypych & Anna (2017). *Databook of Plasticizers*, 2nd ed. Chemtec Publishing, US, 1-3 p.
- [17] Park, H., Misra, M., Drzal, L.T. & Mohanty, A.K. (2004). "Green" nanocomposites from cellulose acetate bioplastic and clay: Effect of eco-friendly triethyl citrate plasticizer, *Biomacromolecules*, Vol. 5(6), pp. 2281-2288. Available: <https://pubs.acs.org/doi/full/10.1021/bm049690f>
- [18] Sinha Ray, S. & Bousmina, M. (2005). Biodegradable polymers and their layered silicate nanocomposites: In greening the 21st century materials world, *Progress in Materials Science*, Vol. 50(8), pp. 962-1079. Available: <https://www.sciencedirect.com/science/article/pii/S0079642505000320>

- [19] Ojijo, V. & Sinha Ray, S. (2013). Processing strategies in bionanocomposites, *Progress in Polymer Science*, Vol. 38(10-11), pp. 1543-1589. Available: <https://www.sciencedirect.com/science/article/pii/S007967001300052X>
- [20] Maheshkumar, K.V., Krishnamurthy, K., Sathishkumar, P., Sahoo, S., Uddin, E., Pal, S.K. & Rajasekar, R. (2014). Research updates on graphene oxide-based polymeric nanocomposites, *Polymer Composites*, Vol. 35(12), pp. 2297-2310. Available: <https://onlinelibrary.wiley.com/doi/full/10.1002/pc.22899>
- [21] Uddin, M.E., Layek, R.K., Kim, N.H., Kim, H.Y., Hui, D. & Lee, J.H. (2016). Preparation and enhanced mechanical properties of non-covalently-functionalized graphene oxide/cellulose acetate nanocomposites, *Composites Part B*, Vol. 90 pp. 223-231. Available: <https://www.sciencedirect.com/science/article/pii/S1359836815007404>
- [22] Ávila-Orta, C.A., Soriano Corral, F., Fonseca-Flórida, H.A., Estrada Aguilar, F.I., Solís Rosales, S.G., Mata Padilla, J.M., González Morones, P., Fernández Tavi-zón, S. & Hernández-Hernández, E. (2018). Starch-graphene oxide bionanocomposites prepared through melt mixing, *Journal of Applied Polymer Science*, Vol. 135(12), pp. 1-8. Available: <https://onlinelibrary.wiley.com/doi/full/10.1002/app.46037>
- [23] Chen, X. (2014). Special Issue of Biopolymers, *Chinese Journal of Chemistry*, Vol. 32(1), pp. 5. Available: <https://doi.org/10.1002/cjoc.201490002>.
- [24] Niaounakis, M. (2015). *Biopolymers: Applications and Trends*, William Andrew, US, pp. 1-3, 42.
- [25] Trinetta, V. (2016). *Biodegradable Packaging*, Reference Module in Food Science, Available: <http://www.sciencedirect.com/science/article/pii/B9780081005965033515>.
- [26] Plackett, D. (2011). Introductory Overview, in: Plackett, D. (ed.), *Biopolymers: New Materials for Sustainable Films and Coatings*, John Wiley & Sons, Incorporated, New York, pp. 10-11.
- [27] Mohanty, A.K., Wibowo, A., Misra, M. & Drzal, L.T. (2004). Effect of process engineering on the performance of natural fiber reinforced cellulose acetate biocomposites, *Composites Part A*, Vol. 35(3), pp. 363-370. Available: <https://www.sciencedirect.com/science/article/pii/S1359835X0300294X>

- [28] Tedeschi, G., Guzman-Puyol, S., Paul, U.C., Barthel, M.J., Goldoni, L., Caputo, G., Ceseracciu, L., Athanassiou, A. & Heredia-Guerrero, J.A. (2018). Thermo-plastic cellulose acetate oleate films with high barrier properties and ductile behaviour, *Chemical Engineering Journal*, Vol. 348 pp. 840-849. Available: <http://www.sciencedirect.com/science/article/pii/S1385894718308209>.
- [29] Vieira, M.G.A., da Silva, M.A., dos Santos, L.O. & Beppu, M.M. (2011). Natural-based plasticizers and biopolymer films: A review, *European Polymer Journal*, Vol. 47(3), pp. 254-263. Available: <http://www.sciencedirect.com/science/article/pii/S0014305710004763>.
- [30] Wypych & George (2017). *Handbook of Plasticizers*, 3rd ed. Chemtec Publishing, US, 24-25 p.
- [31] Dufresne, A. (2012). Cellulose-Based Composites and Nanocomposites, in: Ebnesajjad & Sina (ed.), *Handbook of Biopolymers and Biodegradable Plastics: Properties, Processing and Applications*, William Andrew, St. Louis, pp. 153-154.
- [32] Shchipunov, Y. (2012). Bionanocomposites: Green sustainable materials for the near future, *Pure and Applied Chemistry. Chimie Pure et Appliquee*, Vol. 84(12), pp. 2579-2607. Available: <https://search.proquest.com/docview/2067926588?pq-origsite=summon>
- [33] Dufresne, A., Thomas, S. & Pothan, L.A. (2013). Bionanocomposites: State of the art, Challenges and Opportunities, in: Dufresne, A., Thomas, S. & Pothan, L.A. (ed.), *Biopolymer Nanocomposites: Processing, Properties, and Applications*, Wiley, Somerset, pp. 1-2.
- [34] Shanks, R.A. (2013). Cellulose-Based Nanocomposites: Processing Techniques, in: Dufresne, A., Thomas, S. & Pothan, L.A. (ed.), *Biopolymer Nanocomposites: Processing, Properties, and Applications*, Wiley, Somerset, pp. 391-402.
- [35] Ansari, A. A., Khan, M. N., Alhoshan, M., Aldwayyan, A. S., Alsalhi, M. S. (2010). Nanostructured Materials: Classification, Properties, Fabrication, Characterization and Their Applications in Biomedical Sciences, in: Kestell, A. E. & DeLorey G. T. (ed.), *Nanoparticles: Properties, Classification, Characterization, and Fabrication*, Nova Science Publishers, Incorporated, Hauppauge, pp. 3-4.

- [36] Brody, H. (2012). Graphene, *Nature*, Vol. 483(7389), pp. S29. Available: <https://www.nature.com/articles/483S29a>
- [37] Joshi, R.K., Yoshimura, M. & Kumar, A. (2010). Graphene, *Journal of Nanomaterials*, Vol. 2010(special issue), pp. 1. Available: <https://www.hindawi.com/journals/jnm/2010/915937/>
- [38] Enyashin, A.N. & Ivanovskii, A.L. (2011). Graphene allotropes, *physica status solidi (b)*, Vol. 248(8), pp. 1879-1883. Available: <https://onlinelibrary.wiley.com/doi/full/10.1002/pssb.201046583>
- [39] Novoselov, K.S., Fal'Ko, V.I., Colombo, L., Gellert, P.R., Schwab, M.G. & Kim, K. (2012). A roadmap for graphene, *Nature*, Vol. 490(7419), pp. 192-200. Available: <https://search.proquest.com/docview/1124363874?pq-origsite=summon>
- [40] Kuilla, T., Bhadra, S., Yao, D., Kim, N.H., Bose, S. & Lee, J.H. (2010). Recent advances in graphene based polymer composites, *Progress in Polymer Science*, Vol. 35(11), pp. 1350-1375. Available: <https://www.sciencedirect.com/science/article/pii/S0079670010000699>
- [41] Potts, J.R., Dreyer, D.R., Bielawski, C.W. & Ruoff, R.S. (2011). Graphene-based polymer nanocomposites, *Polymer*, Vol. 52(1), pp. 5-25. Available: <https://www.sciencedirect.com/science/article/pii/S0032386110010372>
- [42] Marcano, D.C., Kosynkin, D.V., Berlin, J.M., Sinitskii, A., Sun, Z., Slesarev, A., Alemany, L.B., Lu, W. & Tour, J.M. (2010). Improved synthesis of graphene oxide, *ACS Nano*, Vol. 4(8), pp. 4806-4814. Available: <https://pubs.acs.org/doi/10.1021/nn1006368>
- [43] Yu, H., Zhang, B., Bulin, C., Li, R. & Xing, R. (2016). High-efficient Synthesis of Graphene Oxide Based on Improved Hummers Method, *Scientific Reports*, Vol. 6(1), pp. 36143. Available: <https://www.nature.com/articles/srep36143>
- [44] Chen, D., Feng, H. & Li, J. (2012). Graphene oxide: Preparation, functionalization, and electrochemical applications, *Chemical reviews*, Vol. 112(11), pp. 6027-6053. Available: <https://pubs.acs.org/doi/10.1021/cr300115g>
- [45] Zhu, Y., Murali, S., Cai, W., Li, X., Suk, J.W., Potts, J.R. & Ruoff, R.S. (2010). Graphene and graphene oxide: Synthesis, properties, and applications, *Advanced*

- Materials, Vol. 22(35), pp. 3906-3924. Available: <https://onlinelibrary.wiley.com/doi/full/10.1002/adma.201001068>
- [46] Luo, D., Zhang, G., Liu, J. & Sun, X. (2011). Evaluation criteria for reduced graphene oxide, *Journal of Physical Chemistry C*, Vol. 115(23), pp. 11327-11335. Available: <https://pubs.acs.org/doi/full/10.1021/jp110001y>
- [47] Pei, S. & Cheng, H. (2012). The reduction of graphene oxide, *Carbon*, Vol. 50(9), pp. 3210-3228. Available: <https://www.sciencedirect.com/science/article/pii/S0008622311008967>
- [48] Park, S., An, J., Potts, J.R., Velamakanni, A., Murali, S. & Ruoff, R.S. (2011). Hydrazine-reduction of graphite- and graphene oxide, *Carbon*, Vol. 49(9), pp. 3019-3023. Available: <https://www.sciencedirect.com/science/article/pii/S0008622311001965>
- [49] Muralisrinivasan & Subramanian, N. (2015). *Basics of Polymers: Fabrication and Processing Technology*, Momentum Press, US, pp. 53, 55.
- [50] Bouvier, J. & Campanella, O. (2014). *Extrusion Processing Technology: Food and Non-Food Biomaterials*, Wiley-Blackwell, GB, pp. 9, 19.
- [51] John R. Wagner Jr, Eldridge M. Mount Iii & Harold F. Giles Jr (2013). *Extrusion: The Definitive Processing Guide and Handbook*, Second ed. William Andrew, US, pp. 3.
- [52] Lafleur, P.G., Vergnes, B., & Reveley, Z. (2014). *Polymer Extrusion*, Wiley-Iste, US, pp. 39-40, 45-47, 109-110.
- [53] Rauwendaal, C. (2014). *Polymer extrusion: Fifth edition*, Hanser, Munich, pp. 15-16.
- [54] Oksman, K., Aitomäki, Y., Mathew, A.P., Siqueira, G., Zhou, Q., Butylina, S., Tanpichai, S., Zhou, X. & Hooshmand, S. (2016). Review of the recent developments in cellulose nanocomposite processing, *Composites Part A: Applied Science and Manufacturing*, Vol. 83 pp. 2-18. Available: <http://www.sciencedirect.com/science/article/pii/S1359835X1500398X>.
- [55] Bendaoud, A. & Chalamet, Y. (2014). Plasticizing effect of ionic liquid on cellulose acetate obtained by melt processing, *Carbohydrate Polymers*, Vol. 108(1),

pp. 75-82. Available: <https://www.sciencedirect.com/science/article/pii/S0144861714002550>

- [56] Riaz, U. & Ashraf, S.M. (2014). Characterization of Polymer Blends with FTIR Spectroscopy, in: Thomas, S., Grohens, Y., & Jyotishkumar, P. (ed.), *Characterization of Polymer Blends: Miscibility, Morphology and Interfaces*, Wiley-VCH, DE, pp. 626-627.
- [57] Murthy, M.S. (2016). X-ray Diffraction From Polymers, in: GUO, Q. (ed.), *Polymer Morphology: Principles, Characterization, and Processing*, Wiley, US, pp. 2197i-j.
- [58] Muller, A.J., Michell, R.M. (2016). Differential Scanning Calorimetry of Polymers, in: GUO, Q. (ed.), *Polymer Morphology: Principles, Characterization, and Processing*, Wiley, US, pp. 4i-j.
- [59] GROENEWOUD, W.M. (2001). CHAPTER 2 - THERMOGRAVIMETRY, in: GROENEWOUD, W.M. (ed.), *Characterisation of Polymers by Thermal Analysis*, Elsevier Science B.V., Amsterdam, pp. 61-76.
- [60] Goldstein, J.I., Newbury, D.E., Echlin, P., Joy, D.C., Lyman, C.E., Lifshin, E., Sawyer, L., Michael, J.R. & SpringerLink (Online service) (2003). *Scanning Electron Microscopy and X-ray Microanalysis: Third Edition*, Springer US, Boston, MA, pp. 37.
- [61] Fei, P.F., Liao, L., Cheng, B.W. & Song, J. (2017). Quantitative analysis of cellulose acetate with a high degree of substitution by FTIR and its application, *ANALYTICAL METHODS*, Vol. 9(43), pp. 6194-6201. Available: <https://pubs.rsc.org/en/content/articlehtml/2017/ay/c7ay02165h>
- [62] Rouf, T.B. & Kokini, J.L. (2016). Biodegradable biopolymer–graphene nanocomposites, *Journal of Materials Science*, Vol. 51(22), pp. 9915-9945. Available: <https://link.springer.com/article/10.1007%2Fs10853-016-0238-4>
- [63] Tian, M., Qu, L., Zhang, X., Zhang, K., Zhu, S., Guo, X., Han, G., Tang, X. & Sun, Y. (2014). Enhanced mechanical and thermal properties of regenerated cellulose/graphene composite fibers, *Carbohydrate Polymers*, Vol. 111 pp. 456-462. Available: <https://www.sciencedirect.com/science/article/pii/S0144861714004858>
- [64] Stobinski, L., Lesiak, B., Malolepszy, A., Mazurkiewicz, M., Mierzwa, B., Zemek, J., Jiricek, P. & Bieloshapka, I. (2014). Graphene oxide and reduced graphene

oxide studied by the XRD, TEM and electron spectroscopy methods, *Journal of Electron Spectroscopy and Related Phenomena*, Vol. 195 pp. 145-154. Available: <https://www.sciencedirect.com/science/article/pii/S0368204814001510>

- [65] Kabiri, R. & Namazi, H. (2014). Nanocrystalline cellulose acetate (NCCA)/graphene oxide (GO) nanocomposites with enhanced mechanical properties and barrier against water vapor, *Cellulose*, Vol. 21(5), pp. 3527-3539. Available: <https://link.springer.com/article/10.1007%2Fs10570-014-0366-4>
- [66] Zhao, X., Zhang, Q.H., Chen, D.J. & Lu, P. (2010). Enhanced Mechanical Properties of Graphene-Based Poly (vinyl alcohol) Composites, *Macromolecules*, Vol. 43(5), pp. 2357-2363. Available: <https://pubs.acs.org/doi/10.1021/ma902862u>
- [67] Uddin, M.E., Layek, R.K., Kim, N.H., Hui, D. & Lee, J.H. (2015). Preparation and properties of reduced graphene oxide/polyacrylonitrile nanocomposites using polyvinyl phenol, *Composites Part B: Engineering*, Vol. 80 pp. 238-245. Available: <http://www.sciencedirect.com/science/article/pii/S1359836815003728>.
- [68] Li, R., Liu, C. & Ma, J. (2011). Studies on the properties of graphene oxide-reinforced starch biocomposites, *Carbohydrate Polymers*, Vol. 84(1), pp. 631-637. Available: <http://www.sciencedirect.com/science/article/pii/S0144861710010271>.